Top Curr Chem (2014) 339: 55–96
DOI: 10.1007/128_2012_359
© Springer-Verlag Berlin Heidelberg 2012
Published online: 6 September 2012

New Insights into the Tropospheric Oxidation of Isoprene: Combining Field Measurements, Laboratory Studies, Chemical Modelling and Quantum Theory

Lisa Whalley, Daniel Stone, and Dwayne Heard

Abstract In this chapter we discuss some of the recent work directed at further understanding the chemistry of our atmosphere in regions of low NO_x, such as forests, where there are considerable emissions of biogenic volatile organic compounds, for example reactive hydrocarbons such as isoprene. Recent field measurements have revealed some surprising results, for example that OH concentrations are measured to be considerably higher than can be understood using current chemical mechanisms. It has also not proven possible to reconcile field measurements of other species, such as oxygenated VOCs, or emission fluxes of isoprene, using current mechanisms. Several complementary approaches have been brought to bear on formulating a solution to this problem, namely field studies using state-of-the-art instrumentation, chamber studies to isolate sub-sections of the chemistry, laboratory studies to measure rate coefficients, product branching ratios and photochemical yields, the development of ever more detailed chemical mechanisms, and high quality ab initio quantum theory to calculate the energy landscape for relevant reactions and to enable the rates of formation of products and intermediates for previously unknown and unstudied reactions to be predicted. The last few years have seen significant activity in this area, with several contrasting postulates put forward to explain the experimental findings, and here we attempt to synthesise the evidence and ideas.

Keywords Hydroxyl radical · Isoprene oxidation · Field measurements · Box model · Biogenic emissions

L. Whalley and D. Heard (✉)
School of Chemistry, University of Leeds, Leeds LS2 9JT, UK

National Centre for Atmospheric Science, University of Leeds, Leeds LS2 9JT, UK
e-mail: D.E.Heard@leeds.ac.uk

D. Stone
School of Chemistry, University of Leeds, Leeds LS2 9JT, UK

Contents

1 Introduction

The composition of the atmosphere is changing, with wide-ranging implications for air quality and climate change. The future well-being of our atmosphere relies on a detailed understanding of the chemistry responsible for the oxidation of man-made and natural emissions. Photo-oxidation in the troposphere is highly complex, and is initiated by short lived radical species, in the daytime dominated by the hydroxyl radical, OH, and at night by the nitrate radical, NO_3, or ozone. Chemical oxidation cycles remove primary emitted trace species which are directly harmful to humans or to the wider environment. The international societal response to deteriorating air quality and the changing climate is guided by the predictions of numerical models which make assumptions about both emission scenarios in the future for trace gases and aerosols from natural and human activity, and global weather patterns which disperse and mix these emissions. An integral part of any air quality or climate model is a chemical mechanism which describes the degradation of all emissions into a wide range of secondary products by reaction with oxidants, for example OH, NO_3, O_3 and Cl atoms, as well as by photochemical degradation by sunlight or removal by physical deposition. Some chemical schemes are very large, containing thousands of individual chemical species and tens of thousands of individual chemical reactions which eventually generate carbon dioxide and water vapour, and along the way a richness of chemical functionality emerges. Many of the secondary products produced by atmospheric photo-oxidation are also directly harmful, for example O_3, NO_2, acids and multifunctional species. Some species are relatively nonvolatile and partition to the aqueous phase to create secondary organic aerosol (SOA) which contributes a significant fraction of tropospheric aerosol, with associated impacts on climate and human health.

It is the realm of laboratory chemical kinetics to measure the rate constants of individual chemical reactions and the yields of products from different reaction channels, under relevant conditions of temperature and pressure, for all processes required to describe adequately chemical oxidation in a given environment. Although very extensive chemical kinetics databases exist for gas phase and heterogeneous reactions, for example from the IUPAC sub-committee for gas kinetic data evaluation [1] (also http://www.iupac-kinetic.ch.cam.ac.uk/), and the JPL kinetics data evaluation panel [2] (also http://jpldataeval.jpl.nasa.gov), and which are used frequently by numerical modellers, there are many gaps, and often the relevant chemistry may be completely missing. Sometimes it is not possible to isolate an individual chemical reaction to study, and process studies in chambers under relevant atmospheric conditions are used to extract kinetic data indirectly. For some reactions it is not possible to synthesise the necessary reagents, and structural–activity relationships (SAR) are used to estimate rate constants using known data from similar molecules and established additivity rules. Estimating the yield of products is more difficult via this method, and theoretical methods utilizing advances in ab initio quantum mechanics have proven extremely useful to predict the likely course of a reaction through calculation of energy barriers to reaction.

Field measurements of atmospheric composition provide crucial data with which to test how complete and accurate chemical mechanisms are within atmospheric models. In the atmosphere, concentrations of trace gases are dependent on the rate of their chemical production and loss, as well as physical transport into or away from the measurement volume. In order to separate chemistry from transport processes, it is useful to measure a species whose chemical lifetime is short, such that transport plays no direct role in controlling its abundance. Free radicals are examples of such species. In steady-state, the abundance of OH is determined by equating the rate of its production and loss, as its rate of loss is directly proportional the concentration of OH. Therefore in order to calculate the abundance of OH it is necessary to measure as wide a range as possible of OH sources and sinks at the same location. Of course, good model-to-measurement agreement for OH may occur fortuitously if missing OH sources counterbalance missing OH sinks in the model. In such cases field measurements have not provided an adequate test of the level of understanding of the underlying chemistry. A common example of missing sinks are some of the many thousands of volatile organic compounds (VOCs) which exist in urban air and which react with OH, and are either directly emitted or generated as reaction intermediates.

Although there are many examples of comparisons between modelled and measured OH, and other radicals, there are relatively few in environments with significant emissions of biogenic volatile organic compounds (BVOCs) at locations which are significantly removed from pollution sources where levels of nitrogen oxides are very low. Chemical mechanisms have been developed for the oxidative degradation of a select few BVOCs, but these schemes are complex, with often only the rate constant of OH with the parent BVOC and the initial branching to primary products well established. The ensuing chemistry involving reactive intermediates and further reactions or photochemistry is often written down, but with relatively little experimental evidence to support the postulated mechanism.

In this chapter we examine the mechanism for the OH initiated oxidation of isoprene under low NO_x levels (NO < 50 ppt). At higher NO_x levels, although it is likely that there are still processes that are missing within atmospheric models (e.g. [3]), isoprene oxidation chemistry is simplified somewhat by the loss of the isoprene-derived peroxy radicals being dominated by reaction with NO. Under low NO_x conditions the fate of these peroxy radicals is much less certain. New insights into the isoprene mechanism have been derived using a combination of:

1. Field measurements of the concentrations of isoprene (and fluxes), OH and HO_2 radicals, and isoprene secondary oxidation products and comparison to calculations of a variety of models, from zero dimensional box models to global three dimensional models.
2. Laboratory studies to study the oxidation of isoprene under carefully controlled conditions, in particular using atmospheric simulation chambers, in order to confirm the presence of reaction products and the rates of competing channels.
3. Theoretical methods using quantum mechanics and chemical rate theory to calculate the multidimensional potential energy surface upon which the reaction of isoprene and OH occurs, and the rates of different reaction pathways under relevant conditions, and the incorporation of these calculated kinetic data into a range of models for comparison with field data.

2 Model and Measurement Comparisons in High Isoprene Low NO_x Regions

A number of field campaigns in regions characterised by high concentrations of isoprene (and sometimes other biogenic species) and low concentrations of NO_x ($NO_x = NO + NO_2$) have highlighted considerable differences between observed and modelled concentrations of OH and HO_2 radicals [4–14]. Appreciable HO_x ($HO_x = OH + HO_2$) concentrations have been observed in the presence of high biogenic emissions that cannot be reconciled with chemical schemes currently adopted in atmospheric models, indicating poor model representation of HO_x chemistry under high VOC and low NO_x conditions. An alternative explanation is that OH and/or HO_2 detected by laser induced fluorescence (LIF) at low pressures [15] may be biased in some way for some instruments in some types of forested environments, for example by the presence of interference under high loadings of isoprene and/or other BVOCs [16, 17].

The earliest reports of model discrepancies for OH and HO_2 under high VOC and low NO_x conditions were made following the aerosols formation from biogenic organic carbon (AEROBIC) campaign in a forested region of Greece in 1997 [5, 18]. The modelled concentrations of OH were, on average, a factor of two lower than the observations, and although the source of the discrepancy was not identified in this study, it was noted that the disagreement was most significant when NO concentrations were low [5].

The program for research on oxidants: photochemistry, emissions and transport (PROPHET) campaign in a deciduous forest in northern Michigan in 1999 also reported OH and HO_2 concentrations that were significantly higher than model calculations, with the OH observations a factor of at least six greater than the modelled concentrations at NO mixing ratios below 100 ppt [12]. This study found that reasonable agreement for OH could be obtained if the NO concentrations in the model were tripled, or the NO doubled and the isoprene halved, indicating the combination of low NO_x and high isoprene as a source of the problem [12].

The suggestion that incomplete or incorrect treatment of reactions involving organic peroxides (ROOH), either their formation via $HO_2 + RO_2$ or their photolysis to produce RO + OH, may be responsible for the HO_x model failure came as a result of the southern oxidant study (SOS) in Nashville, Tennessee [13]. At high NO_x concentrations the dominant fate of HO_2 and RO_2 is generally reaction with NO, resulting in production of OH, either directly (in the case of HO_2) or via the production of an alkoxy radical (RO) and its subsequent reaction with O_2 (in the case of RO_2). Any misrepresentation of $HO_2 + RO_2$ reactions, or their products, in model simulations will therefore become more apparent at low NO_x concentrations owing to the reduced importance of HO_2 + NO and RO_2 + NO reactions.

2.1 Recycling of OH in Isoprene Oxidation

The Guyanas atmosphere–biosphere exchange and radicals intensive experiment with the Learjet (GABRIEL) project carried out in 2005 reported the first boundary layer measurements of OH and HO_2 made over a tropical rainforest, with measurements made over the Amazon rainforest in Suriname onboard a Learjet aircraft using LIF [9]. Global models predict particularly low OH concentrations in this region due to elevated levels of isoprene which rapidly reacts with OH [19–21], but comparison with the GABRIEL dataset revealed significant differences between model predictions and observations [4, 7, 8]. Disagreements between observed and modelled OH concentrations for GABRIEL were found with both global models [4] and box models [7], with the OH concentrations simulated by the box model, constrained to the reduced Mainz isoprene mechanism (MIM), a factor of approximately 12 times lower than the observations at the highest isoprene concentrations. Use of a more explicit isoprene oxidation scheme, similar to that described by the master chemical mechanism (MCM), did little to improve the model failure [7].

The OH model discrepancy for GABRIEL was found to display a dependence on isoprene [4, 7, 8], as shown in Fig. 1. This discrepancy was similar to that observed over forested regions in North America, in the intercontinental chemical transport experiment (INTEX-A), and during the PROPHET campaign [10] (also shown in Fig. 1). The level of discrepancy between OH observed and predicted from other isoprene-rich field studies (Oxidant and Particle Photochemical Processes – OP3 and Program of Regional Integrated Experiments of Pearl River Delta region – PRIDE-PRD, discussed further below) were also consistent with this trend.

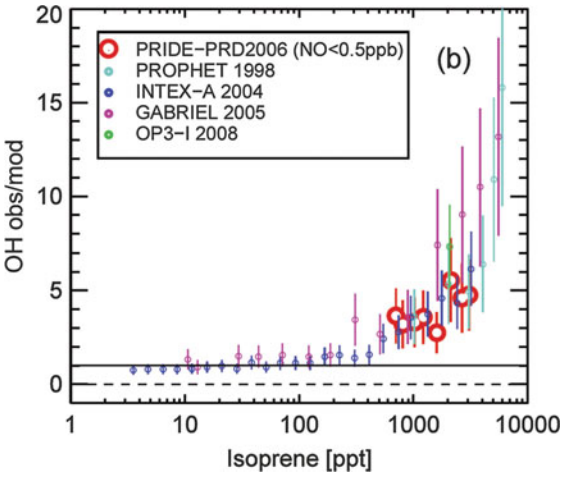

Fig. 1 Dependence of the observed to modelled ratio for OH as a function of the isoprene mixing ratio reported from PROPHET (1998), INTEX (2004), GABRIEL (2006), PRIDE-PRD (2006) and OP3-I (2008) projects (reproduced from Lu et al. [57])

Isoprene photo-oxidation products were also found to be higher than model predictions [22], indicating the need for additional OH sources related to isoprene in order to reconcile models with measurements. This observation led to an extension of the idea that reactions involving HO_2 and RO_2 could be responsible for model failure. It was proposed that direct formation of OH in $HO_2 + RO_2$ reactions, and specifically those involving RO_2 radicals generated in isoprene oxidation ($ISOPO_2$), could improve model simulations for OH over the Amazon rainforest by providing an additional pathway for recycling of OH via HO_2 under low NO_x conditions, as shown in Fig. 2 [4, 7, 8].

Generation of OH in $HO_2 + RO_2$ reactions has been observed in several laboratory studies [23–28], and although inclusion of an OH yield in $HO_2 + ISOPO_2$ reactions in atmospheric models has enabled replication of field observations, the yields required (between 200% and 400%) are significantly higher than the laboratory data suggest for any reaction of this type. Moreover, production of OH in such reactions has thus far only been observed for RO_2 radicals containing acyl, α-carbonyl, α-hydroxy or α-alkoxy functionalities [23–28], and experiments have placed an upper limit of 6% on the OH yield from RO_2 radicals structurally similar to $ISOPO_2$ [23].

2.2 *The Role of Air Mass Segregation in Simulations of HO_x Chemistry*

While the production of such large amounts of OH from $HO_2 + RO_2$ reactions is unlikely, its inclusion in atmospheric models does facilitate investigation of the impact of underpredictions of OH in modelling studies. Butler et al. [4] found that increasing the OH concentration in a global 3D model European centre for medium-range weather forecasts-Hamburg/module earth submodel system

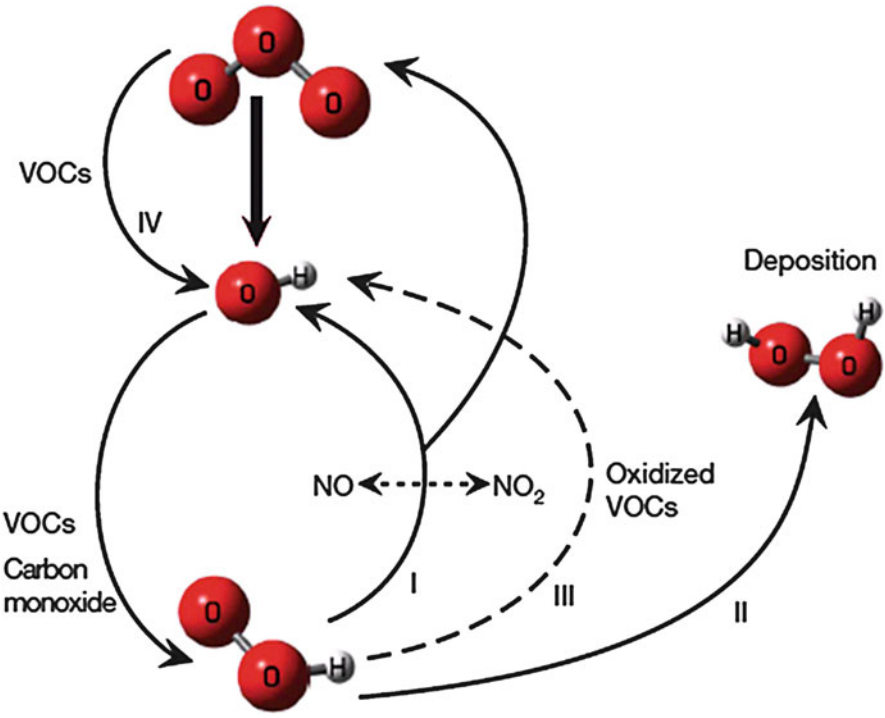

Fig. 2 Schematic to show the main processes controlling HO_x concentrations in the troposphere (reproduced from [8]). Pathway I shows the cycling of HO_2 to OH through reaction with NO; pathway II shows the production of peroxides from HO_2, leading to loss of HO_x; pathway III indicates a potential route for production of OH from reactions of HO_2 with VOC oxidation products

(ECHAM/MESSy) led to unrealistically low concentrations of isoprene. In order to achieve model agreement with observed concentrations of both OH and isoprene it was necessary not only to include the additional OH source but also to reduce the effective rate coefficient between OH and isoprene by approximately 50% [4]. The rationale behind the reduction in $k_{OH+C_5H_8}$ lies in the potential segregation of air masses containing OH from those containing isoprene, such that the two air masses do not fully mix and therefore do not react at a rate given by $k_{OH+C_5H_8}[OH][C_5H_8]$ when considering the concentrations of OH and isoprene in the two air masses.

This concept has also been investigated by Pugh et al. [29, 30] for the OP3 project which took place in Borneo in 2008, comprising both ground-based and aircraft measurements of atmospheric composition in and over rainforest and oil palm plantations [31]. Using the Cambridge tropospheric trajectory model of chemistry and transport (CiTTyCAT) atmospheric chemistry box model with MIM2 chemistry, Pugh et al. [29] demonstrated similar problems in simulating OH concentrations to those reported by Lelieveld et al. [8], with the model unable

to replicate concurrent observations of OH and isoprene whilst maintaining agreement with measurements of VOC emission fluxes.

Pugh et al. [29] included a recycling term for OH in the reaction between OH and isoprene to investigate its impact on the model simulations, but found that any improvements in the modelled OH were at the cost of model success for isoprene and other VOCs. Further analysis of the model revealed that reasonable agreement with observations could be achieved for OH and VOCs by a combination of a small recycling term in OH, variation of the deposition rates of intermediate VOC oxidation products, including methyl vinyl ketone (MVK) and methacrolein (MACR), and segregation of OH-containing and isoprene-containing air masses. Similar to the work of Butler et al. [4], Pugh et al. [29] represented the segregation of air masses containing OH from those containing isoprene by a reduction in the effective rate coefficient for the OH + isoprene reaction, with a 50% reduction required to achieve adequate model success. It was thus concluded that model success in tropical regions may be less strongly influenced by mechanistic problems in isoprene oxidation schemes than by detailed representation of physical and micrometeorological processes. This conclusion is in contrast to those of Whalley et al. [14] and Stone et al. [11], discussed below, which conclude that mechanistic changes can result in significant differences in modelled HO_x concentrations for the OP3 campaign.

The importance of boundary layer dynamics and potential segregation of oxidant-rich and VOC-rich air parcels has also been investigated using a large eddy simulation within a mixed-layer model [32]. Although the model uses a highly condensed gas phase chemistry mechanism containing only 19 reactions, the results of the study suggest that the chemistry is equally important as the dynamics in reproducing isoprene mixing ratios measured during the tropical forest and fire emissions experiment (TROFFEE) campaign in Central Amazonia in 2004.

The extent of segregation and turbulent mixing above a forest canopy has been estimated using tower-based measurements of OH, HO_2 and VOC above a deciduous forest in Germany during the emission and chemical transformation of biogenic volatile organic compounds (ECHO) campaign in conjunction with the eddy covariance method [33]. This study showed that, although inhomogeneous mixing can occur near emission sources, the degree of segregation of air masses observed was significantly less than that required to improve the model simulations for the Amazon rainforest [4] and the Borneo rainforest [29]. A reduction in the effective rate coefficient for OH + isoprene of 15% was justified by the measurements [33], in contrast to the 50% proposed by Butler et al. [4] and Pugh et al. [29].

In addition, Pugh et al. [30] conducted a model analysis of high frequency isoprene measurements, made by a proton transfer reaction-mass spectrometer (PTR-MS) instrument during the OP3 campaign in Borneo, to provide an experimentally-based estimate of the extent of segregation between OH and isoprene during OP3. To test the analysis method, Pugh et al. [30] analysed data taken during the German ECHO project and determined similar percentage segregations of OH and isoprene as reported by Dlugi et al. [33]. When applied to the OP3 dataset, Pugh et al. [30] found that the 50% reduction in the effective rate coefficient for the OH + isoprene reaction required to reconcile model discrepancies could not be justified. The results indicated that a

maximum reduction of 15% in the effective rate coefficient for reaction between OH and isoprene was more appropriate, suggesting that the chemistry may play a more significant role than expected by Pugh et al. [29].

Further evidence for a limited role of air mass segregation in explaining OH model discrepancies in tropical regions has been provided by Ouwersloot et al. [34] using a large eddy simulation model. Ouwersloot et al. [34] propose that incomplete mixing of reactive species in a turbulent boundary layer over a spatially homogeneous surface should reduce the OH + isoprene rate coefficient by no more than 10%, while spatially heterogeneous surface emissions should result in no more than a 20% reduction in OH + VOC effective rate coefficients [34]. Comparing model simulations with homogeneous surface emissions to those with heterogeneous emissions yielded differences in OH concentrations of <2% [34]. Several papers thus suggest a limited role of turbulent mixing and segregation of air masses in explaining observed OH concentrations [30, 33, 34].

3 Unidentified Sources of OH in High Isoprene Environments

The possibility for production of OH through unknown chemistry was discussed by Hofzumahaus et al. [6] as a potential explanation for model underestimates of OH in the Pearl River Delta region in China. This study demonstrated the ability of a box model to reproduce HO_2 observations whilst underestimating OH observations by a factor of up to 5, and postulated the presence of an unknown species able to convert RO_2 to HO_2 and HO_2 to OH independently of NO and without producing ozone. Although the region surrounding the Pearl River Delta is characterised by high biogenic VOC emissions, the noontime NO mixing ratios were significantly higher than those encountered during the GABRIEL and OP3 projects (~200 ppt at noon for the Pearl River Delta compared to ~20 ppt for the GABRIEL and OP3 campaigns). Nevertheless, the OH discrepancies were consistent with other field studies which encountered similarly elevated isoprene concentrations (as shown in Fig. 1), suggesting that problems with isoprene oxidation mechanisms can lead to model failures even under moderate NO_x conditions.

Further evidence for the involvement of isoprene oxidation chemistry in model failures in low to moderate NO_x regions has also come from laboratory and theoretical studies, revealing that the oxidation mechanisms currently adopted in atmospheric models provide inaccurate representations of isoprene-related photochemistry, with model discrepancies more likely to be apparent under low NO_x conditions.

3.1 Experimental Indication for OH Formation During Isoprene Oxidation

A chamber study by the California Institute of Technology (CalTech) group observed epoxide formation during the gas phase Photo-oxidation of isoprene [35], with

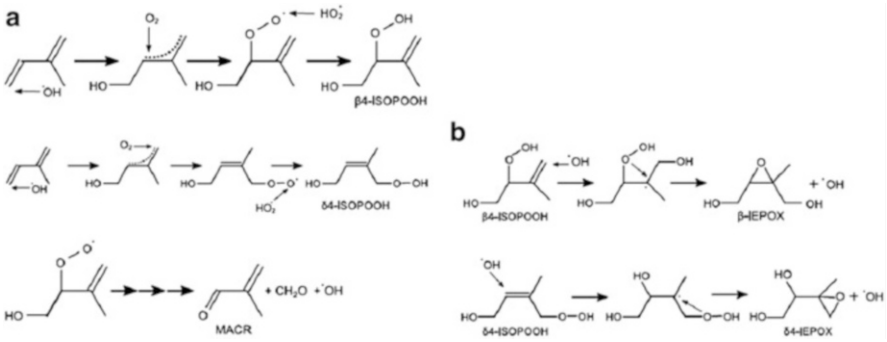

Fig. 3 (**a**) Production of peroxides (ISOPOOH) and MACR following OH-addition to isoprene in the atmosphere. (**b**) Formation of epoxides following addition of OH to isoprene peroxides (reproduced from [35])

implications for OH production and generation of SOA. The CalTech environmental chamber produces OH by photolysis of H_2O_2, resulting in low NO_x conditions (initial mixing ratios of NO_x were varied between 0.1 and 1.3 ppb), and uses a chemical ionisation mass spectrometry (CIMS) detection system to monitor stable reaction products of the OH + isoprene reaction. The experiments showed that peroxides (ISOPOOH) were formed in high yields following OH addition to isoprene and the subsequent reaction of peroxy radicals ($ISOPO_2$) with HO_2, with smaller reaction channels resulting in production of OH, formaldehyde and either MACR or MVK (depending on the site of the initial OH addition to isoprene). The reaction scheme depicting these processes is shown in Fig. 3a and Table 1 provides the structural formulas for abbreviations of isoprene-derived species discussed in Sects. 3.2 and 3.3.

Production of peroxides and MVK/MACR following OH-addition to isoprene has been observed in previous studies [36–38], and is included in chemical mechanisms such as the MCM [39]. Prior to the CalTech study, the ISOPOOH peroxides were expected to undergo physical loss, photolysis (yielding ISOPO alkoxy radicals and OH) or react with OH to produce a peroxy radical (in the case of the dominant ISOPOOH isomer of the four isomers in the MCM) or carbonyl species with regeneration of OH (in the case of the three remaining ISOPOOH isomers in the MCM).

However, the CalTech group showed that the reaction of ISOPOOH peroxides with OH could produce epoxides (IEPOX) in an OH neutral reaction, as shown in Fig. 3b. Although the IEPOX species are isobaric with ISOPOOH, and thus appear as a combined IEPOX + ISOPOOH CIMS signal, use of collision induced dissociation enables the production of distinct daughter ions from each compound and separation of the signals. Use of ^{18}OH also enabled separation of the IEPOX and ISOPOOH signals, since ISOPOOH requires addition of one ^{18}OH on isoprene, whereas IEPOX production involves addition of a second ^{18}OH to ISOPOOH and loss of a ^{16}OH radical. Theoretical arguments also provide

Table 1 Abbreviations and structural formulas associated with isoprene oxidation products

Isoprene oxidation products	Structural formula
β4-ISOPO$_2$	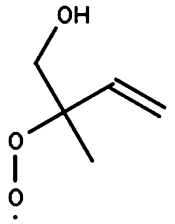
δ4-ISOPO$_2$	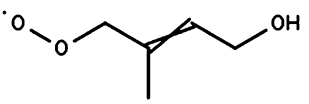
β4-ISOPOOH	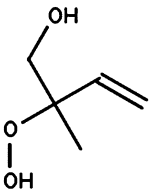
δ4-ISOPOOH	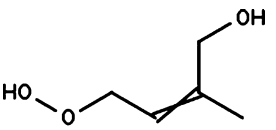
β4-IEPOX	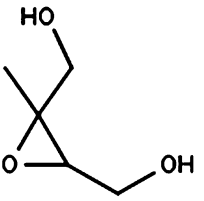
δ4-IEPOX	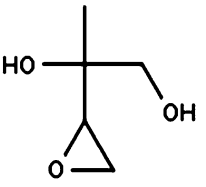

(continued)

Table 1 (continued)

Isoprene oxidation products	Structural formula
β4-ISOPO	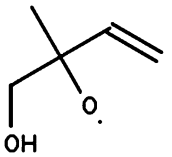
δ4-ISOPO	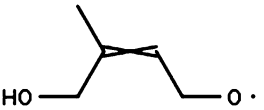
β4-HPALD	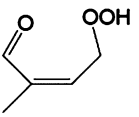
δ4-HPALD	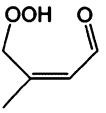
β4-PACALD	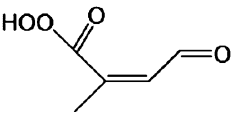
HALD	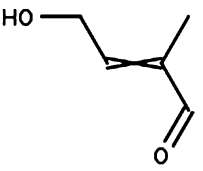
MVK	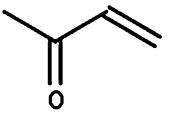
MACR	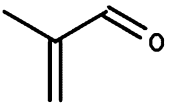

evidence for the existence of an energetically favourable pathway producing IEPOX from ISOPOOH [35].

While the initial epoxide production from ISOPOOH is OH-neutral, and will thus have little impact on modelled OH concentrations in low NO_x environments, the discovery of IEPOX species highlights significant gaps in our understanding of isoprene oxidation chemistry. Moreover, the fate of the IEPOX species may be important in terms of understanding field observations of OH and formation of SOA. It is expected that the lifetime of IEPOX with respect to OH addition is of the order of 18–22 h, and that reactive uptake of IEPOX to aerosol surfaces and subsequent SOA formation could be important [35]. If IEPOX are involved in SOA formation then isoprene-derived carbon will be sequestered from the gas phase, potentially reducing the expected impact of isoprene on atmospheric OH concentrations.

The production of ISOPOOH, and therefore IEPOX, is dependent on the reaction of $ISOPO_2$ radicals with HO_2, and is thus expected to occur to a greater extent in low NO_x regions. However, recent theoretical studies have indicated that $ISOPO_2$ radicals may undergo unimolecular decomposition processes which do not produce ISOPOOH, but may result in regeneration of HO_x radicals [40–43].

3.2 *Theoretical Indication for OH Production in Isoprene Oxidation*

Density functional theory (DFT) calculations have predicted the unimolecular decomposition of β-$ISOPO_2$ radicals (the dominant $ISOPO_2$ isomers), resulting in production of OH, formaldehyde and (depending on the isomer) MVK or MACR [40]. However, the rates of decomposition are expected to be slow, and may not be sufficient to compete effectively with the bimolecular reactions of $ISOPO_2$ radicals with HO_2 and NO in all but the most remote environments [40].

Theoretical investigation of the OH-initiated oxidation of isoprene by the Leuven group has also led to the proposal of HO_x radical production following unimolecular processes in $ISOPO_2$ radicals [41–43]. An outline of the initial steps in the proposed mechanism – the Leuven isoprene mechanism (LIM) – are shown in Fig. 4.

A key feature of the mechanism is the existence of an equilibrium between the initial OH-isoprene radical adduct and the $ISOPO_2$ peroxy radical formed on addition of molecular oxygen to the adduct, leading to the greatest reaction flux through the fastest product forming pathway [42]. Under low NO_x conditions, Peeters et al. [42] propose that the fastest pathways occur through unimolecular 1,6-H shifts in two of the $ISOPO_2$ radicals, producing HO_2 and unsaturated hydroperoxy-aldehydes (HPALDs). Based on an average temperature of 303 K and concentrations of 5×10^8 cm^{-3} NO (~20 ppt), 10^9 cm^{-3} HO_2 (~40 ppt) and 10^9 cm^{-3} total RO_2, Peeters et al. [42] calculated a value of 0.025 s^{-1} for

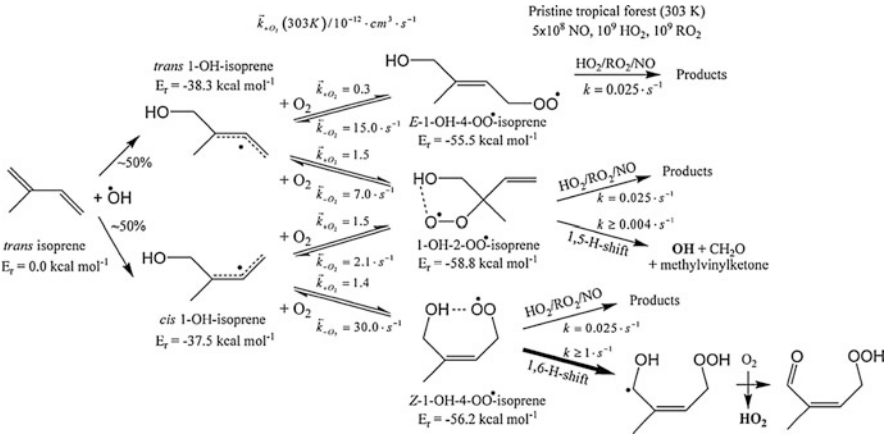

Fig. 4 Outline of the initial steps in the Leuven Isoprene Mechanism, with their predicted rates, following 1-OH addition to isoprene (reproduced from [42])

$\{k_{NO}[NO]+k_{HO_2}[HO_2]+k_{RO_2}[RO_2]\}$ (where k_x is the rate coefficient for the reaction of $ISOPO_2$ isomers with species X). In comparison, the proposed $ISOPO_2$ isomerisation processes to produce the HPALD and HO_2 were expected to occur with $k \geq 1\ s^{-1}$ for the $ISOPO_2$ isomer produced by 1-OH addition to isoprene and $k \geq 8\ s^{-1}$ for the $ISOPO_2$ isomer produced following 4-OH addition.

The HPALD products are thought to photolyse rapidly during the day, owing to the combination of the –OOH hydroperoxide moiety and an O=C–C=C chromophore, thereby increasing the yield of both OH and HO_2 [42]. Subsequent chemistry of the organic fragments of HPALD photolysis, resulting in rapid production of photolabile peroxy-acid-aldehydes (PACALDs), is also expected to increase further the OH and HO_2 yields [41–43]. More minor reaction pathways of the initial $ISOPO_2$ peroxy radicals, involving 1,5-H shifts, are also proposed to contribute to OH production, and the potential for similar mechanisms in the oxidation of MVK and MACR has been postulated [42] and, in the case of MACR, experimentally verified [44].

3.3 Experimental and Theoretical Evidence for OH Production Combined

Peeters and Müller [43] surveyed available experimental evidence in order to assess the strengths of the LIM, comparing the expected yields of key species in the novel mechanism against those derived from previous work. Figure 5 shows the dependence of a number of these key species (OH, HPALD, HALD, MVK and MACR) as a function of the NO mixing ratio as derived from the LIM and used in the analysis by Peeters and Müller.

Mechanisms, such as the MCM or MIM, currently adopted in atmospheric models predict relatively high concentrations of hydroxy aldehydes (HALDs),

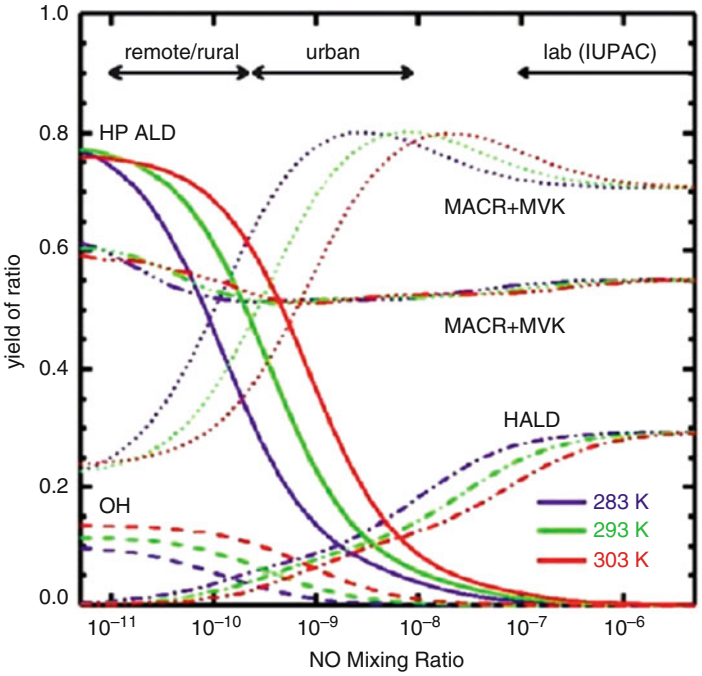

Fig. 5 Expected yields of key species in the Leuven Isoprene Mechanism as a function of the NO mixing ratio (reproduced from [43])

largely formed by hydroxy alkoxy ISOPO radicals produced in $ISOPO_2$ + NO reactions. Such HALDs, however, have yet to be observed in the field or in laboratory studies at NO mixing ratios below 1 ppb [43]. Peeters and Müller provide an example of this in the work of Karl et al. [37], in which a MIM-based mechanism would predict HALD yields of over 40% in their photoreactor study at NO mixing ratios between 200 and 600 ppt. The LIM predicts a maximum HALD yield of 5% at 400 ppt NO, as shown in Fig. 5, and the lack of HALD observations at low NO mixing ratios is put forward in support of the LIM [43].

Peeters and Müller [43] also discussed the results of the CalTech chamber study [35] in the context of the LIM, proposing that a significant proportion of $ISOPO_2$ sinks were unaccounted for in the CalTech experiment, which could potentially be explained by the additional 1,6-H shifts predicted by the LIM.

The CalTech study observed combined [MVK + MACR] yields of approximately 12% in the absence of NO, attributable to the minor $ISOPO_2$ 1,5-H shift channels [43]. Although this yield is somewhat higher than predicted by the LIM, requiring a factor of 5 increase in the predicted 1,5-H shift rate coefficients, this increased yield does help to rectify discrepancies in MVK/MACR ratios between the LIM and field observations of Karl et al. [22] made in the Amazon rainforest.

The rate coefficients calculated for LIM by Peeters et al. [42] were stated to be lower limits, owing to a possible underestimation of the effects of tunnelling.

Peeters and Müller [43] proposed a similar argument to explain the low rates of peroxy radical isomerisation processes calculated by da Silva et al. [40], and discussed the uncertainties associated with the LIM calculations in greater detail. The probable error on the rates of peroxy radical isomerisations was reported to be of the order of a factor of 5, owing to possible errors on the calculated dissociation energies and barrier heights, and thus within the bounds of the increase required to reconcile the theory with the CalTech experiments. Moreover, calculations made using higher levels of theory indicated that the computed barrier heights for the isomerisation reactions were lower than had been initially reported, supporting the expectation that the calculated rates represent a lower limit.

Low observed yields of a product with a CIMS signal consistent with the HPALD products in the CalTech study were explained by Peeters and Müller [43] as resulting from high chamber concentrations of HO_2, making ISOPOOH peroxide formation more favourable than the unimolecular process generating the HPALDs. In addition, photolysis of HPALDs in the chamber, coupled with their reaction with OH, is expected to have led to more rapid HPALD loss ($\sim 4 \times 10^4\ s^{-1}$) compared to ISOPOOH loss ($\sim 6.4 \times 10^{-5}\ s^{-1}$).

Very recently the photo-oxidation of HPALDs was incorporated into a detailed chemical mechanism and embedded into a global atmospheric model which generated higher levels of OH in better agreement with field measurements in pristine forested regions [45].

Further work by the CalTech group [46] has provided more direct evidence for the formation of HPALDs in isoprene oxidation, and hence for the occurrence of rapid 1,6-H shifts in $ISOPO_2$ radicals. The experiments were designed to investigate the OH-initiated oxidation of isoprene in the chamber at concentrations of HO_2 and NO pertinent to the pristine troposphere, with NO mixing ratios ranging between 30 and 60 ppt, using photolysis of methyl nitrite (CH_3ONO) as the HO_x source. The study was conducted over a range of temperatures, with experiments also performed using fully deuterated isoprene (C_5D_8) in order to corroborate conclusions drawn from the C_5H_8 system.

The HPALD production rates were measured relative to those of H_2O_2, produced by the HO_2 self-reaction, and ISOPOOH, produced by $HO_2 + ISOPO_2$ [46]. It was therefore possible to determine the ratio of the rate coefficient for the 1,6-H shift in $ISOPO_2$ ($k_{1,6\text{-H}}$) relative to that for $HO_2 + ISOPO_2$ ($k_{HO2+ISOPO2}$), using literature recommendations for the HO_2 self-reaction rate coefficient. This method does, however, require knowledge of the CIMS sensitivity to the measured species. For H_2O_2 the sensitivity can be determined using gas phase standards, but it was necessary for HPALD and ISOPOOH sensitivities to be calculated [46].

The experimental analysis did not consider oxidation chemistry of the reaction products (H_2O_2, ISOPOOH, HPALD), introducing a potential error of $<10\%$ [46]. Photolysis of the HPALD product was expected to be negligible under the experimental conditions [46].

The results of the study provide clear evidence for the formation of HPALDs, and thus for the 1,6-H shifts in $ISOPO_2$ radicals predicted by Peeters et al. [42]. However, the rate of HPALD formation was observed to be approximately 50 times

slower than that expected by Peeters et al. [42] and Peeters and Müller [43]. Implementation of the 1,6-H shifts in $ISOPO_2$ radicals into the global 3D chemistry transport model GEOS-Chem showed that while the isomerisation reaction producing HPALDs is an important process in isoprene oxidation, constituting 7.4% of the global loss of $ISOPO_2$ radicals, the reaction is not as dominant as previously expected [46]. Recent work by the CalTech group has demonstrated that isomerisation reactions in other organic peroxy radicals can also lead to OH formation, with OH observed following a rapid 1,4-H shift in a peroxy radical derived from MACR [44]. The impact of these novel OH sources on model simulations is considered below.

4 Impacts of Additional OH Sources on Model Simulations in High Isoprene Low NO_x Regions

Several studies have been conducted to assess the impact of the potential mechanistic changes in isoprene oxidation on tropospheric concentrations of OH and HO_2, including our own work as part of the OP3 project in Borneo [11, 14, 31].

Wolfe et al. [47] used the one-dimensional chemistry of atmosphere – forest exchange (CAFE) model – to aid understanding of measurements made during the biosphere effects on aerosols and photochemistry experiment (BEARPEX-2007) campaign in a Ponderosa pine forest in the western foothills of the Sierra Nevada Mountains in California. The chemistry scheme within the model was based on MCMv3.1, with additional chemistry to represent the formation of isoprene-derived epoxides as observed by Paulot et al. [35]. However, the model still underpredicted OH observations by a factor of 6 during particularly warm periods when VOC emissions were high [47]. During these 'hot' periods, Wolfe et al. [47] required additional OH sources, which were represented in the model by the production of OH from $HO_2 + RO_2$ reactions, similar to the modelling studies for the GABRIEL campaign [4, 7, 8]. Formation of epoxides in isoprene oxidation, although an important discovery in terms of our understanding of isoprene chemistry, thus appears to do little to rectify model discrepancies for OH.

This result has also been observed in a number of other modelling studies [11, 47–49]. Stavrakou et al. [49] used the intermediate model of global evolution of species IMAGESv2 global chemistry transport model to investigate the impacts of several of the previously described proposed mechanisms for OH recycling in isoprene oxidation. The model used chemistry based on the MIM2 [50], with simulations to assess the impacts of the artificial recycling scheme used by Lelieveld et al. [8] and Wolfe et al. [47], the formation of isoprene epoxides and the occurrence of $ISOPO_2$ 1,6-H shifts in the LIM. It was found that the LIM had the greatest potential for increasing modelled HO_x concentrations over densely vegetated areas in the tropics and at mid-latitudes, with increases in OH concentrations by a factor of 4 compared to the MIM2. In comparison, inclusion

of epoxide forming chemistry gave increases in OH by a factor of only 1.25. As described by Stavrakou et al. [49] and Peeters and Müller [43], inclusion of the LIM in the IMAGESv2 model replicated average boundary layer observations of OH and HO_2 during the GABRIEL and INTEX campaigns to within 30%.

Archibald et al. [48] also investigated the impacts of OH formation from $HO_2 + RO_2$ reactions, epoxide chemistry, and 1,5-H and 1,6-H shifts in $ISOPO_2$ radicals, using a zero-dimensional model with chemistry based on the MCMv3.1. Inclusion of OH-producing channels in $HO_2 + RO_2$ reactions in which OH formation is expected to occur gave increases in OH concentrations of 7%, compared to a 16% increase on consideration of the epoxide chemistry and 330% for the 1,5-H and 1,6-H shifts in $ISOPO_2$.

Implementation of a modified version of CRIv2-R5 chemistry scheme [51] within the UK meteorological office three-dimensional Lagrangian global model (STOCHEM) indicated that use of the LIM resulted in significant elevations in modelled OH concentrations over rainforested regions in the Amazon and in Borneo, and concluded that the LIM had the greatest potential for increasing modelled OH concentrations. It was noted, however, that it was likely that some degree of parameter refinement and optimisation within the scheme would be necessary before the mechanism could be fully reconciled with atmospheric observations and other laboratory data.

While arguments to explain some of the apparent discrepancies between laboratory data and the LIM may have been put forward by Peeters and Müller [43], it would appear that there are outstanding issues in modelling HO_x observations with the mechanism as it currently stands. In our work as part of the OP3 project in Borneo [31], measurements of OH and HO_2 were made by both ground-based instruments in the rainforest [14, 52] and by an aircraft instrument on the BAe146 NERC research aircraft [11]. Analysis of the HO_x observations and detailed chemical modelling with the dynamically simple model of atmospheric chemical complexity (DSMACC) [53] for both ground and aircraft campaigns have revealed that HO_x observations in tropical regions still cannot be fully explained.

The combination of measurements of HO_x concentrations and the OH reactivity (a measure of the total OH sinks in an air mass) [52, 54] at the ground-based site enabled quantification of the total OH source in the rainforest [14]. It was found that to maintain the observed OH concentrations, given the measured reactivity, required an OH production rate ten times greater than that calculated using all measured OH sources. Model calculations were also shown to under-predict simultaneously the observed OH concentrations while over-predicting HO_2. Inclusion of an additional OH source formed as a recycled product of OH-initiated isoprene oxidation improved the model agreement for OH, but served to worsen the model failure for HO_2. In order to replicate observations of both OH and HO_2, the model required additional loss process for HO_2, or a process that converts HO_2 to OH.

OP3 aircraft measurements have also been used to test our understanding of isoprene oxidation chemistry, using the DSMACC box model to assess the ability of the various proposed oxidation mechanisms to reproduce the observed

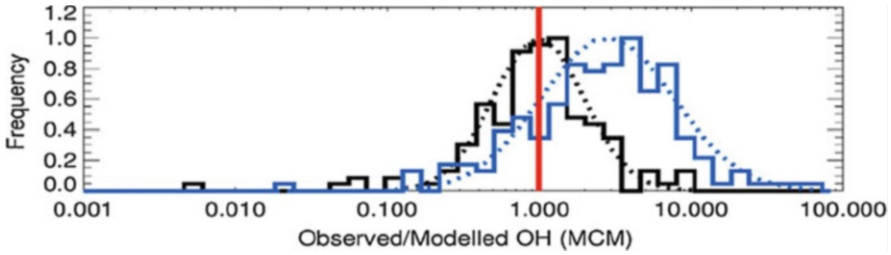

Fig. 6 Probability distribution functions of the observed to modelled ratio for OH using the MC**Mv3**.1 for data points during the OP3 aircraft campaign with low (<15 ppt) isoprene concentrations (*black*) and high (>15 ppt) isoprene concentrations (*blue*), with Gaussian fits to the data shown by the *broken lines*. The *red line* indicates an observed to modelled ratio of 1. The plot displays the ability of the model to replicate OH observations at low isoprene concentrations, but a model failure at high isoprene concentrations (reproduced from [11])

concentrations of OH and HO_2 [11]. The base model run for the aircraft campaign, using the MCMv3.1, displayed a significant underestimate for OH in airmasses impacted by isoprene, with a mean observed to modelled ratio of $5.32^{+3.68}_{-4.43}$ compared to a ratio of $1.62^{+1.27}_{-1.24}$, for airmasses not significantly impacted by isoprene, as shown in Fig. 6 [11]. For HO_2, the model was generally able to replicate the observations, with no significant dependence of the model success on the isoprene concentration.

Table 2 shows the OP3 aircraft model results for the range of potential isoprene oxidation mechanisms and additional OH sources discussed above, including epoxide formation [35], unimolecular decomposition of isoprene peroxy radicals [41–43] and recent updates to the MCM (MCMv3.2). In keeping with the results of Whalley et al. [14], the LIM gave significant improvements to the modelled OH concentrations, but resulted in a large model overestimate for HO_2. However, the experimental findings of Crounse et al. [46], indicating a slower HPALD production rate than predicted by Peeters et al. [42] and Peeters and Müller [43], reduces the impact of the LIM and thus its potential to rectify model discrepancies for OH.

Analysis of our measurements during OP3 [11, 14] show that it is not possible to remove simultaneously the model bias in both OH and HO_2 using any of the suggestions described above. The results of this field campaign show that, despite significant recent advances in our understanding of isoprene oxidation chemistry, there are still considerable gaps in our knowledge. Similar conclusions have been drawn from field studies in anthropogenically influenced regions under high isoprene loadings [6, 55–58], indicating that uncertainties in the isoprene oxidation mechanism are important not only under pristine forest conditions (NO < 50 ppt), but also at moderate NO_x levels (several hundred ppt) in populated areas where ozone production and air quality predictions could be biased. Lu et al. found that the LIM mechanism was unable to reconcile fully OH observed during PRIDE [57] and CAREBeijing2006 (Campaigns of Air Quality Research in Beijing and Surrounding Region 2006) [58], particularly if the reduced isomerisation rate determined by

Table 2 Mean observed to modelled ratios of OH and HO_2 at isoprene concentrations above and below 15 ppt for a range of mechanisms investigated by Stone et al. [11]

Mechanism	Mean $[OH]_{obs/mod}$, $C_5H_8 < 15$ ppt	Mean $[OH]_{obs/mod}$, $C_5H_8 > 15$ ppt	P_D	P_H	Mean $[HO_2]_{obs/mod}$, $C_5H_8 < 15$ ppt	Mean $[HO_2]_{obs/mod}$, $C_5H_8 > 15$ ppt	P_D	P_H
MCMv3.1	$1.62^{+1.27}_{-1.24}$	$5.32^{+3.68}_{-4.43}$	0	0	$0.86^{+0.32}_{-0.31}$	$1.18^{+0.30}_{-0.30}$	0	0.921
MCMv3.2	$1.62^{+1.27}_{-1.24}$	$4.51^{+3.08}_{-3.75}$	0	0	$0.83^{+0.31}_{-0.31}$	$1.05^{+0.27}_{-0.27}$	0	0.889
$C_5H_8 + OH \rightarrow 3OH$	$1.62^{+1.27}_{-1.24}$	$1.62^{+1.25}_{-1.25}$	0.867	0.054	$0.86^{+0.32}_{-0.31}$	$0.67^{+0.30}_{-0.26}$	0	0
$HO_2 + ISOPO_2 \rightarrow 3OH$	$1.62^{+1.27}_{-1.24}$	$1.62^{+1.11}_{-1.21}$	0.913	0.149	$0.86^{+0.32}_{-0.31}$	$0.70^{+0.21}_{-0.21}$	0	0
$HO_2 + RO_2 \rightarrow 0.5OH$	$1.42^{+1.14}_{-1.07}$	$4.13^{+2.87}_{-3.39}$	0	0	$0.81^{+0.30}_{-0.30}$	$1.05^{+0.27}_{-0.27}$	0	0
$RO_2 + X \rightarrow HO_2$ $HO_2 + X \rightarrow OH$	$1.62^{+1.27}_{-1.24}$	$1.68^{+0.38}_{-1.49}$	0	0.001	$0.86^{+0.32}_{-0.31}$	$0.89^{+0.40}_{-0.40}$	0.002	0
Epoxide	$1.62^{+1.27}_{-1.24}$	$4.27^{+2.90}_{-3.52}$	0	0	$0.86^{+0.32}_{-0.31}$	$0.96^{+0.24}_{-0.24}$	0	0.633
da Silva	$1.62^{+1.27}_{-1.24}$	$5.19^{+4.31}_{-3.61}$	0	0	$0.86^{+0.32}_{-0.31}$	$1.17^{+0.30}_{-0.30}$	0	0.943
Peeters	$1.62^{+1.27}_{-1.24}$	$1.50^{+1.12}_{-1.14}$	0.820	0.014	$0.86^{+0.32}_{-0.31}$	$0.46^{+0.18}_{-0.19}$	0	0

Errors shown are the standard deviations in the mean. P_D refers to the probability result of a Kolmorogov–Smirnov test and refers to the probability that the distribution functions of the ratios for data points with isoprene above and below 15 ppt are statistically identical. P_H refers to the probability result of a Kruskal–Wallis test and indicates the probability that the ratios for data points with isoprene concentrations above 15 ppt are independent of the isoprene concentration. Probability values <0.001 are listed as zero (reproduced from [11])

Crounse et al. [46] was implemented; inclusion of epoxide chemistry also had little impact on the modelled OH in these studies. Inclusion of LIM led to overpredictions of HO_2 measured during PRIDE, CAREBeijing2006 and HOxCOMP [55–58] similar to findings from OP3.

Archibald et al. [59] investigated the impact of HO_x recycling in isoprene oxidation on modelling of past, present and future atmospheres using the UKCA global chemistry climate model. The study showed the potential for substantial changes to our estimates of global methane lifetimes as a result of developments in our understanding of isoprene chemistry. The changes to OH concentrations owing to changes to the descriptions of isoprene chemistry result in an 11% reduction in the global methane lifetime and a 9% increase in the global ozone burden by 2100. The representation of isoprene chemistry in atmospheric models thus has important consequences for predictions of future climate change scenarios.

The role of isoprene chemistry in controlling atmospheric composition and climate, and the influence of temperature and land use change on isoprene emissions, should not be underestimated. The field observations of OH in isoprene-rich, NO_x-poor environments discussed above indicate that isoprene has a considerably smaller effect on OH concentrations than chemistry models predict. This conclusion, based on direct measurements of OH and comparison with model predictions, is also supported by observations of other atmospheric species undertaken in VOC rich NO_x poor environments. Discrepancies between isoprene concentration measurements and model predictions when constrained to isoprene emission inventories have been reported, as have discrepancies between model predictions of isoprene oxidation product concentrations and those measured. Large model underestimates of OH reactivity and SOA formation under isoprene-rich conditions also point towards significant uncertainties in the OH-initiated isoprene oxidation mechanism.

5 Isoprene Emission Rates and Mixing Ratios and Comparisons with Model Predictions

Emission inventories of natural VOCs on regional and global scales have been available since the late 1970s. Many of the regional and global early inventories [60–62] suffered from considerable weaknesses owing to lack of available/relevant data including accurate estimates of global vegetation coverage, VOC emissions from different sources, how emissions change with changes in drivers such as temperature and light intensity and how these drivers change [63]. With these weaknesses in mind, considerable effort was put into generating a more robust global emission inventory on a $1^\circ \times 1^\circ$ grid for use in global chemistry and transport models. The global emissions inventory activity (GEIA) developed a model of isoprene and other VOC emissions [63] and a regional biogenic emissions model [biogenic emissions inventory system (BEIS)] developed in the 1980s [64] was updated [65]. The model of emissions of gases and aerosols from nature

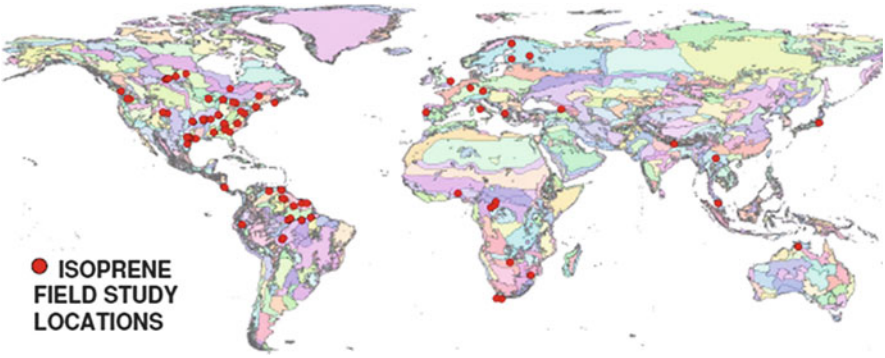

Fig. 7 Geographical distribution of ecoregions identified in Olson et al. [138] and the locations of ~90 isoprene field experiments used to develop isoprene emission factors (reproduced from [66])

(MEGAN) was developed to replace GEIA and BEIS in 2006 [66]. The isoprene emission rates recommended in the mid-1990s [63, 65] were greater by more than a factor of two than those previously used in the early regional air quality and global transport models [60–62, 64]. Global emission estimates of isoprene were of the order of 570 Tg year^{-1} and were derived primarily from enclosure measurement studies which assigned leaf level emission factors to many global ecosystems; other ecosystems that were unmeasured were assigned default values. In the GEIA and BEIS inventories only 3 of the 20 publications used to determine emissions included studies conducted in tropical regions. In addition to this, emission activity algorithms describing the response of isoprene emissions to temperature and light were based on investigations of temperate plants rather than tropical measurements [63].

Since the 1990s, thousands of isoprene emission rate measurements using enclosure techniques have been conducted (Fig. 7) and are incorporated into the most recent global emission inventories [66]. These are often extrapolated to canopy scale using canopy environment models. Measurements conducted in tropical regions are now much more abundant [67–72] and direct measurements of above-canopy fluxes have become more widespread, enabling parameterisation of emissions on an eco-system scale, e.g. [73, 74], which is particularly advantageous in tropical landscapes where eco-system species are extremely diverse. With much improved constraints, MEGAN estimates a global isoprene emission of ~600 Tg year^{-1}. In many cases, when employed in chemistry and transport models and global atmospheric chemistry models, these isoprene emission rates result in unrealistically high concentrations of isoprene and ozone in the boundary layer [75, 76]. Scaling factors have been introduced in many instances which uniformly reduce emissions by 20% or more or, in some cases, reduce emissions in selected landscapes by up to a factor of 3 [77]. The intergovernmental panel on climate change (IPCC) recommends a 56% reduction in global isoprene emission rates as recommended by Guenther et al. [63] to allow models to replicate observations of

CO and isoprene concentrations [78]. Favourable comparisons between canopy-scale emissions based on leaf-level emission measurements and above-canopy flux measurements scaled up (or down) with a canopy environment model have been made, however. Spirig et al. [79] found that above-canopy fluxes of isoprene measured using eddy covariance and PTR-MS during the ECHO campaign, which took place in a European deciduous forest, provided a top-down estimate of isoprene emission rates at the leaf level comparable to cuvette measurements made at the site. Similarly, Kuhn et al. [80], measuring isoprene and monoterpene fluxes in a tropical forest in the Central Amazon basin, found that the observed VOC fluxes were in good agreement with simulations using a single-column chemistry and climate model (SCM). Comparison of the biogenic emission model, MEGAN, with flux measurements made in the Amazon basin during TROFFEE were also found to agree with each other within associated model and measurement uncertainties [81].

Discrepancies between flux observations and emission models have been reported; these differences tend to relate to the use of inappropriate base emission rates (BER) (rate at which plants emit isoprene under a set of standard conditions; $T = 30°C$; photosynthetically active radiation = 1,000 μmol m^{-2} s^{-1}) within emission models, however. Langford et al. (2010) report isoprene and monoterpene flux observations made during OP3. Comparison of the observations with emissions estimated by the MEGAN model demonstrated that large discrepancies could arise if default isoprene BER – based on measurements (Fig. 7, Table 3) made over the Amazon rainforest where the emission factors are largely derived from – were used, with model isoprene emissions being four times greater than those observed. The modelled to measured flux agreement could be improved considerably, however, if the model was constrained to typical photosynthetically active radiation (PAR) and temperature variables measured at the Borneo station [82]. Hewitt et al. [83] have recently demonstrated that BER for isoprene is not necessarily constant and instead is under circadian control and can vary throughout the day. Assuming a constant BER led to an overestimation in the isoprene flux relative to those observed during OP3 [83]. These direct flux observations and comparison to emission models suggest that emissions inventories do not necessarily overestimate isoprene emission rates; rather, other model factors such as deposition of isoprene oxidation products, oxidation schemes employed or the factors controlling isoprene emissions may contribute to poor model performance [66].

It must be noted that, although the examples given above demonstrate good agreement between modelled emissions rates and directly measured isoprene fluxes, many of these models overestimate VOC mixing ratios [76, 77]. For example, Kuhn et al. [80] observed the vertical gradients of isoprene and isoprene oxidation products; comparison between model and observations led Kuhn and co-workers to suggest that the oxidation capacity was much higher than that assumed by the model. A simple chemical kinetics study utilising the ratio of (MVK + MACR)/isoprene estimated an [OH] of ~8×10^6 molecule cm^{-3}, an order of magnitude higher than predictions made by the model employed. This high [OH]

Table 3 Isoprene and monoterpene flux measurements from tropical forests and typical monoterpene: isoprene ratio (units in mg C $m^{-2} h^{-1}$; reproduced from Langford et al. 2010 [82]). See Langford et al. [82] for details of the references cited in this table

Location	Season	Method	Isoprene	∑Monoterpene	Ratio	References
Borneo SE Asia	L wet	vDEC	0.48 ± 0.72	0.13 ± 0.19	0.27	Langford et al. (this study)
Borneo SE Asia	E dry	vDEC	1.04 ± 1.3	0.25 ± 0.33	0.24	Langford et al. (this study)
Malaysia SE Asia	Dry	LL	1.1	–	–	Saito et al. (2008)
Amazon, Brazil	E dry	MB	2.7	0.24	0.23	Zimmerman et al. (1998)
Amazon, Peru	E dry	MLG	7.2	0.45	0.06	Helmig et al. (1998)
Amazon, Brazil	L wet	EC, REA	2.1	0.23	0.11	Rinne et al. (2002)
Amazon, Brazil	L dry	vDEC	7.3 ± 2.7	1.5 ± 1.1	0.21	Karl et al. [81]
Amazon, Brazil	L dry	MLG	10.2 ± 3.5	2.2 ± 0.7	0.22	Karl et al. [81]
Amazon, Brazil	L dry	MLV	11.0 ± 0.9	3.9 ± 1.1	0.35	Karl et al. [81]
Amazon, Brazil	E dry	REA	2.1 ± 1.6	0.39 ± 0.43	0.19	Kuhn et al. [80]
Amazon, Brazil	E dry	SLG	3.4 ± 3.6	0.38 ± 0.58	0.11	Kuhn et al. [80]
Amazon, Brazil	–	REA	1.1	0.2	0.18	Stefani et al. (2000)
Amazon, Brazil	–	BM	1.9	0.16	0.08	Greenberg et al. (2004)
Amazon, Brazil	–	BM	4.7	0.20	0.04	Greenberg et al. (2004)
Amazon, Brazil	–	BM	8.6	0.54	0.06	Greenberg et al. (2004)
Amazon, Brazil	Dry	EC	0.4–1.5	–	–	Muller et al. (2008)
Amazon, Brazil	Wet	EC	0.1–0.3	–	–	Muller et al. (2008)
French Guyana Suriname	Dry	CBL	6.1	–	–	Eerdekens et al. (2009)
Costa Rica	Wet	REA	2.2	–	–	Geron et al. (2002)
Costa Rica	Dry	DEC	2.2	0.29	0.13	Karl et al. [74]
Congo, Africa	–	A-REA	0.9	–	–	Greenberg et al. (1999)
Congo, Africa	–	LL	0.8–1	–	–	Klinger et al. (1998)
Congo, Africa	–	REA	0.46–1.4	–	–	Serca et al. (2001)

EC eddy convariance, *vDEC* virtual disjunct eddy convariance, *DEC* disjunct eddy convariance, (*A*)-*REA* (airborne) relaxed eddy accumulation, *SLG* surface layer gradient, *MB* mass budget, *MLG* mixed layer gradient, *MLV* mixed layer variance, *LL* leaf level extrapolation, *BM* box modelling, *CBL* convective boundary layer budgeting

estimate was also supported by a simple budget analysis, which assumes that the isoprene mixing ratio is in steady state with the chemical boundary layer and, hence, the amount of isoprene emitted and entrained (F_{ISO}) is balanced by the

amount chemically degraded by oxidants such as OH and O_3 at a particular boundary layer height (z_i). The respective flux-to-lifetime relationship can be described as

$$F_{\mathrm{ISO}} = (k_{\mathrm{OH(ISO)}} \times [OH] + k_{\mathrm{O_3(ISO)}} \times [O_3]) \times [ISO] \times z_i. \quad (1)$$

Solving (1) for OH, Kuhn and co-workers estimate an OH radical concentration of ~4.5×10^6 molecule cm^{-3} using mean observations of isoprene mixing ratios and fluxes determined using mixed layer gradient measurements. These elevated OH concentration estimates support the recent, direct, OH concentration measurements made over Suriname [8]. Increasing the modelled OH concentration was suggested to remedy isoprene emissions with the observed isoprene concentrations [80]. Similarly, Karl et al. [81] found during a study conducted during the dry season in the Amazon that OH modelled in the boundary layer using a photochemical box model was significantly lower than that calculated using the mixed layer budget analysis. Karl et al. [81] hypothesised that reactive sesquiterpenes present at 1% of the isoprene concentration could produce sufficient OH radicals by ozonolysis (assuming an OH yield of one) that could largely reconcile the differences in the OH predicted by a zero dimensional detailed chemical box model and estimates based on the budget analysis.

Pugh et al. [29], using a box model to simulate the atmospheric boundary layer over the Borneo rainforest, constrained to the measured VOC fluxes [82], found that the model, rather than overpredict isoprene (as is the case with many of the earlier emission constrained models), was able to simulate concentrations well, but underpredicted the measured OH concentration (by two to three times) and over-predicted the concentrations of isoprene oxidation products of MVK and MACR considerably (five to ten times) (consistent with findings by Kuhn et al. [80] and Karl et al. [81]). Increasing the dry deposition velocity of the MVK and MACR improved the modelled to measured agreement for these species and brought the modelled OH into better agreement with observations due to a reduction in the modelled OH sink. Pugh et al. [29] found that increasing OH in the model only served to reduce the modelled isoprene concentration, with modelled isoprene concentrations dropping below those observed. Increasing the isoprene emissions (to greater than observed) to rectify the model underestimation only resulted in a further re-suppression of OH [29]; Butler et al. [4] report similar findings from model measurement comparisons undertaken as part of the GABRIEL project. As discussed in Sect. 2.2, Pugh et al. found that a 50% segregation between OH and isoprene was able to reconcile inconsistencies between measurements, although in a later paper Pugh et al. [30] determined the degree of segregation explicitly for observations conducted during OP3 and concluded that the segregation was not >15%. These findings highlight that, despite an accurate representation of isoprene emissions, observations of isoprene, isoprene oxidation products and OH cannot be fully reconciled, suggesting that there are still gaps in our understanding of isoprene oxidation chemistry.

5.1 Isoprene Emissions Inferred from Satellite Measurements of HCHO

Global and regional biogenic emissions, determined using bottom-up methods which rely on as yet relatively sparse in-situ concentration data (Fig. 7) and/or flux measurements extrapolated to regional or continental scales using satellite-derived land cover, have large associated uncertainties. For example, the annual global isoprene emission estimated with MEGAN ranges from 500 to 750 Tg isoprene depending on driving variables such as temperature, solar radiation, leaf index area and plant functional type [66]. A promising, alternative approach for assessing global emission inventories and developing global isoprene emission maps is to use a top-down approach based on satellite measurements of isoprene oxidation products such as formaldehyde (HCHO). The success of this technique to predict global isoprene emissions accurately relies heavily on an accurate description of isoprene oxidation leading to the formation of HCHO and upon the OH concentration, however. The principal sink of isoprene is oxidation by the OH radical; underestimating OH concentrations will directly affect isoprene and HCHO concentrations. The method assumes that the HCHO column, Ω (molecule cm^{-2}), observed by satellites, and the sum of HCHO precursor emissions at steady state in the absence of horizontal transport can be linearly related by

$$\Omega = \frac{1}{k_{\mathrm{HCHO}}} \sum_i Y_i E_i \tag{2}$$

where k_{HCHO} is the first order loss of HCHO from oxidation and photolysis applied to the column, E_{i} is the emission of VOC species i and Y_i is the HCHO yield from species i. For isoprene the conversion time to HCHO may be as little as 1 h and the lifetime of HCHO is of the order of a few hours during the daytime. For reactive VOCs, such as isoprene, which produce HCHO promptly, transport away from the point of emission can be considered minimal and, as such, any variability in the HCHO column can be assumed to be largely caused by variability in isoprene oxidation rather than transport into and out of the HCHO column. Fu et al. [84] compared observed HCHO columns from the global ozone monitoring experiment (GOME) satellite with those simulated using the Goddard Earth Observing System chemical transport model (GEOS-Chem) constrained to biogenic emissions determined using MEGAN [66]. Isoprene emissions from east and south Asia inferred from the satellite measurements were 53 ± 30 Tg $year^{-1}$ and compared well, on average, with MEGAN predictions of 56 Tg $year^{-1}$ for the region. MEGAN was found to underestimate isoprene emissions by a factor of 3 for Chinese mixed forests and croplands and overestimate emissions from tropical vegetation. Using a similar approach, Millet et al. [85] studied the spatial distribution of HCHO over North America, using HCHO column measurements taken from the ozone monitoring instrument (OMI), and compared to the bottom-up MEGAN emission inventory. Although spatially consistent, OMI-derived isoprene emissions were

found to be between 4% and 25% lower than those predicted by MEGAN on average. Shim et al. [86] used the GEOS-Chem chemical transport model driven by the GEIA biogenic emissions database to conduct a global inversion of GOME HCHO column data. The estimated global isoprene annual emissions were higher at mid-latitudes and lower in the tropics when compared to the GEIA inventory. Barkley et al. [87] comparing isoprene emissions derived from HCHO GOME columns and those derived from the MEGAN inventory found that over South America MEGAN predicted much higher isoprene emissions than GOME; this positive bias was found to be larger in the dry season than the wet season. The mean [OH] from MEGAN and GOME simulations conducted by Barkley et al. [87] were approximately 1.2–4.5 lower than values observed over the tropical rainforest in Suriname during the GABRIEL project. Underestimating the OH oxidation in the GOME model will in turn lead to an underestimation of isoprene inferred from the observed HCHO column. Additional OH recycled during isoprene oxidation could help to resolve quantitatively MEGAN and GOME isoprene emission estimates [87].

6 Isoprene Oxidation Products

Observations of other isoprene oxidation products such as MVK, MACR and hydroxyacetone in a number of field studies and comparison with model predictions also point towards large uncertainties in isoprene oxidation schemes currently employed. Observed oxygenated volatile organic carbon (OVOC) mixing ratios are determined by a balance of their production (largely dominated by photochemistry) and loss rates (which include reactive loss, dry deposition and vertical mixing). Pugh et al. [29], for example, found that the model scheme used to assess chemistry during the OP3 project that took place in the Borneo rainforest greatly overestimated the sum of MVK and MACR measured and suggested that the dry deposition rate of these OVOC could be larger than assumed by the model. Karl et al. [22], comparing observations of MVK + MACR and hydroxyacetone (measured using PTR-MS) during the Amazonian aerosol characterisation experiment (AMAZE-08) with model predictions, report a factor of 10 underprediction in the hydroxyacetone/(MVK + MACR) ratio, implying a missing source of hydroxyacetone in the model. Karl et al. [22] also reanalysed data from five other field campaigns and found that during all of them, hydroxyacetone mixing ratios were significantly higher than what would be expected from model predictions which assume that the major source of hydroxyacetone is an oxidation product of MACR. Theoretical studies have proposed a primary source of hydroxyacetone direct from isoprene [88], and laboratory studies have demonstrated a fast secondary production which is currently not included in atmospheric chemistry models [3]. Karl et al. [22] implemented the additional hydroxyacetone pathway proposed by Paulot et al. [3] extended to low NO_x conditions in model runs and found that the mechanism reproduced well the MVK/MACR ratio observed during

the AMAZE campaign; the modelled hydroxyacetone/(MVK + MACR) ratio obtained from the Paulot mechanism was within 50% of observations, suggesting that fast secondary production could explain 50% of the observed hydroxyacetone/(MVK + MACR) ratio. The remaining 50% may be related to the primary production mechanism as suggested by [88]. Karl et al. [22] also assessed the performance of the recently proposed Leuven mechanism in reproducing the AMAZE OVOC observations. This mechanism was found to predict an MVK/MACR ratio of ~10; observed ratios were typically ~1.34 (measured by GC-MS). The Leuven mechanism also significantly underestimated the sum of MVK and MACR to isoprene ratio. The yields of MVK, MACR and hydroxyacetone are highly sensitive to the rate of decomposition of the 1,6-H shift reactions which are proposed to be rapid in the Leuven mechanism (Fig. 4). Karl et al. [22] found that to reconcile the mechanism of Leuven with the observed OVOC ratios during the AMAZE campaign would require the 1,6-H shift reactions decomposition rate and the reverse reaction rates of the *Z*-1-OH-4-OO* and *Z*-4-OH-1-OO* peroxy radicals to be reduced (consistent with the experimental results of Crounse et al. [46]). Such an adjustment would lead to a corresponding reduction in the overall HO_x yield from the Leuven mechanism, with an approximate yield of 0.1 HO_2 and 0.12 OH radicals, just 33% of the original.

7 OH Reactivity

If, as suggested by Karl et al. [22], the rate of formation of isoprene oxidation products are underestimated, due to uncertainties in the isoprene oxidation method employed in models, this will undoubtedly impact the oxidative capacity and OH reactivity determined by models due to reaction of these OVOCs with OH. Although the direct radiative forcing of these species is small, their indirect effect on the lifetime of species such as CH_4 and their role in the formation of organic aerosol and tropospheric ozone have an important influence on climate as well as local and regional air quality [89]. Observations of the total OH reactivity have been made in a variety of chemical environments [52, 54, 90–101]. In most studies the observed reactivity is underestimated by models constrained to the measured OH sink species; this discrepancy is often greatest in regions of high biogenic activity [52]. Much of this discrepancy may be caused by unmeasured VOCs using standard observation techniques such as gas chromatography [102]. Chung et al. [103] found that as much as 45% of the total non-methane organic carbon was unmeasured during observations in the Los Angeles basin. The discrepancy increased as the air mass aged, suggesting that the missing organic fraction was made up largely by oxidation products of primarily emitted VOCs. In contrast to this, Di Carlo et al. [90] found that the oxidation products of the VOCs observed in a mid-latitude mixed hardwood forest accounted for <2% of the calculated OH reactivity and instead suggested that unmeasured primarily emitted biogenic

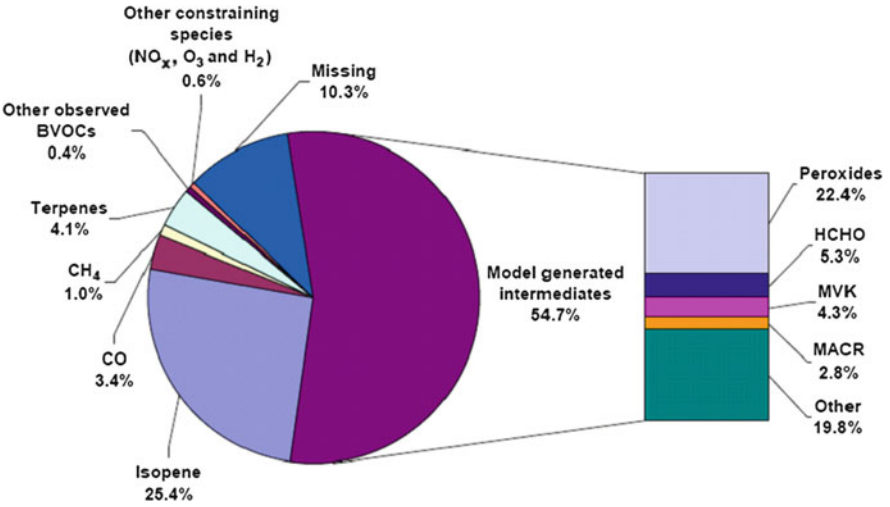

Fig. 8 Pie-chart showing the contributions to OH reactivity calculated using a zero-dimensional box model constrained to the Master Chemical Mechanism for comparison with observations of OH reactivity made during the OP3 campaign in the Borneo rainforest

VOCs such as terpenes could account for the missing reactivity. Di Carlo et al. [90] relied on a heavily lumped model, however.

Sinha et al., [100] determined during measurements taken in Suriname, within the canopy at a height of approximately about 35 m, an average OH reactivity of ~53 s^{-1} with a peak OH reactivity of 72 $\pm$ 18 s^{-1}. The calculated OH reactivity determined from concentration measurements of acetone, acetaldehyde, isoprene, MVK and MACR made up just 35% of the measured OH sink; the limited dataset, however, prevented any strong conclusions on the likely missing sink species. Edwards et al. [52] assessed the measured OH reactivity observed in the Borneo rainforest using a zero dimensional model based upon MCM chemistry and found that the model was particularly sensitive to concentrations of unconstrained oxidation products of the observed BVOCs, in particular isoprenal hydroperoxides, carbonyls and alcohols, highlighting the importance of these species in the chemistry controlling oxidation in this environment. This importance of isoprene oxidation products as a major sink for tropical OH has been suggested previously by Warneke and Gouw [104], where measured concentrations of MVK, MACR and isoprenal peroxides above the Amazon rainforest resulted in large reductions in OH concentrations within a photochemical box model. Edwards et al. [52] demonstrate from direct measurements of OH and OH reactivity within a tropical rainforest that as much as 55% of the observed OH loss is potentially through reaction with unmeasured oxidation products of primary BVOCs. This work highlights the importance of an accurate description of the isoprene degradation mechanism within models to understand ultimately the fate of the oxidised isoprene products and their impact on the oxidising capacity (Figs. 8 and 9).

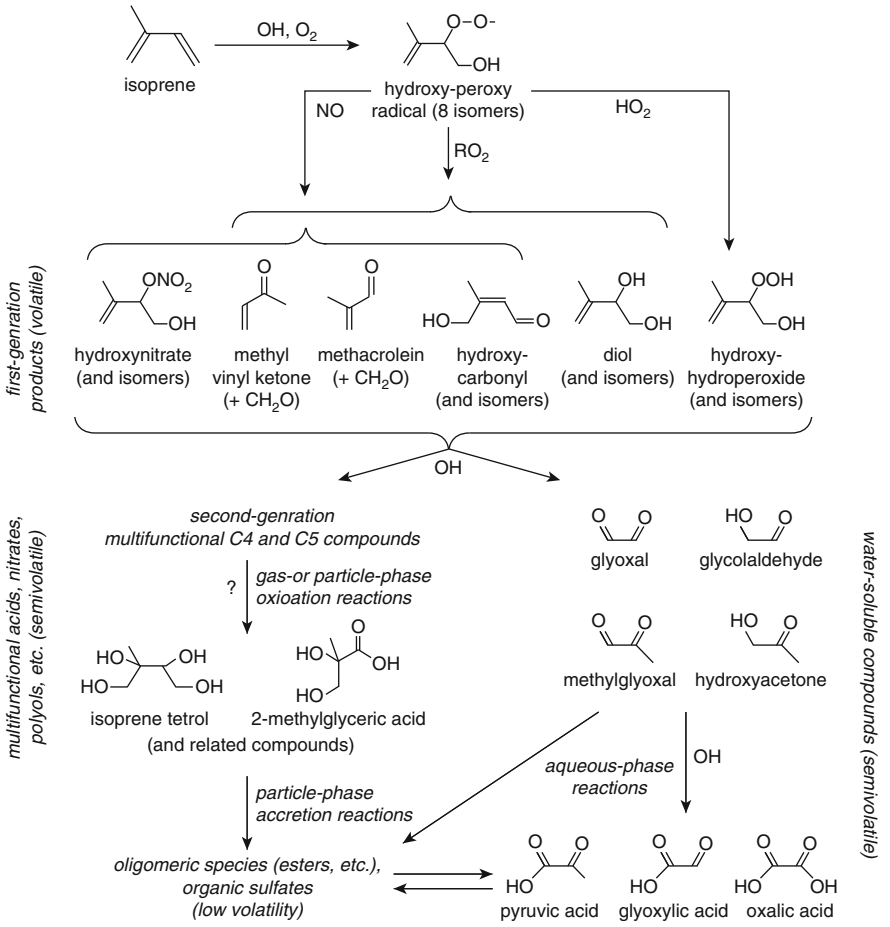

Fig. 9 Oxidation pathways leading to isoprene SOA (reproduced from [137])

8 SOA Formation from Isoprene

The oxygenated products of isoprene may contribute to SOA formation and, as such, any uncertainty in the isoprene oxidation mechanism will impact model predictions of SOA. Atmospheric models consistently underpredict organic aerosol mass in both the boundary layer and aloft [105–111]. This underprediction is not present in model predictions of black (elemental) carbon, leading to the conclusion that this bias is due to an underprediction in SOA specifically. Although isoprene is one of the most abundant hydrocarbons emitted into the atmosphere, second only to methane [63], in the early 1990s it was concluded that isoprene did not form SOA through gas-phase oxidation owing to the assumption that SOA only forms when condensable products reach concentrations exceeding their saturation vapour pressure [112]. In support of

this, early chamber studies only observed SOA formation from isoprene at concentrations much greater than ambient levels [113–115]. Kiendler-Scharr suggests that the presence of isoprene may actually suppress SOA formation from mono-terpene oxidation [116] owing to the scavenging of OH by isoprene (and the assumed lack of SOA formation from isoprene oxidation). In contrast, offline field measurements of organic aerosol in forested areas indicated that isoprene did play a part in SOA formation [117–123]. Claeys et al. [118] detected considerable quantities of methyl tetrols which have the isoprene skeleton in organic aerosols from the Amazon rainforest. The authors estimated that the photo-oxidation of isoprene may result in the global production of 2 Tg year^{-1} of the polyols, a significant fraction of the total IPCC estimate of SOA from biogenic sources of 8–40 Tg year^{-1}. Laboratory studies have now demonstrated that absorption into condensed-phase organics could provide a mechanism for SOA formation from gas-phase species at concentrations below their saturation vapour pressure [115, 124]. In 2003 Limbeck and co-workers proposed that isoprene, by direct reaction with acidic particles, was able to contribute to the formation of humic-like substances that make up 20–50% of the water-soluble organic aerosols in urban and rural European air [125]. The most recent results from laboratory and chamber studies indicate that isoprene oxidation can form SOA even in the absence of a strong seed aerosol [126–128], albeit over longer timescales [129]. Isoprene derived SOA species (e.g. epoxides, tetrols and organosulphates) have now been measured in chamber studies [35, 123, 130–132] and observed in the offline field samples. Kiendler-Scharr et al. [133], by introduction of fully deuterated isoprene into plant chambers containing non-isoprene emitting poplars, determined an aerosol mass yield from isoprene of ~2.3%. Online SOA field observations made, for example, using aerosol mass spectrometry, which provide higher time-resolved data and permit comparison to gas-phase isoprene oxidation products and fast changing oxidant concentrations, have recently been reported. During OP3, Robinson et al. [134] observed that up to 15% by mass of the sub-micron organic aerosol was observed as methyl furan in the aerosol mass spectrum (AMS) and was assigned to be representative of isoprene SOA owing to the simultaneous observation of gas-phase isoprene oxidation products of MVK and MACR. Froyd et al. [135], using online particle analysis by laser mass spectrometry (PALMS), also observed isoprene-derived SOA in the form of IEPOX-derived organosulphates, a second generation oxidation product of isoprene. From this study it was estimated that IEPOX contributed >0.4% to tropospheric aerosol mass in the remote tropics and up to 20% in regions downwind of isoprene sources [135].

The distribution of isoprene oxidation products depends upon the fate of the RO_2 radicals formed. Upon reaction with NO, MVK and MACR and hydroxynitrates may form; conversely, under low NO_x conditions hydroxyhydroperoxides form by reaction of RO_2 with HO_2. SOA yields under low NO_x conditions tend to be higher than under higher NO_x scenarios (~3% yield vs 1–2% yield at higher NO_x concentrations) [128], suggesting that further reactions of the hydroxyhydroperoxides can lead to lower volatility products. Surratt and Kroll and co-workers have found that the oxidation of MACR generates SOA with very similar chemical

composition to SOA formed from isoprene, suggesting that MACR is an important intermediate in the formation of SOA from isoprene [128, 131]. Henze and Seinfeld [136] demonstrated that inclusion of an SOA source from isoprene increased the SOA yield in global model simulations considerably but the increase alone was not sufficient to reconcile observations made during the ACE-Asia campaign [106]. Currently a single-step process for SOA formation from isoprene is assumed within most atmospheric models used to estimate SOA formation [137]. The kinetic study by Ng et al. [129], however, highlighted the multi-oxidation nature of SOA formation from isoprene as it was found that most of the aerosol formation observed only occurred after most of the isoprene was consumed. Carlton and co-workers [137] suggest that modelling SOA formation from the individual isoprene products may better reflect the multi-step nature of isoprene oxidation and SOA formation, but an improved understanding of the chemical mechanisms involved in isoprene oxidation is needed before this can be implemented.

9 Summary

Uncertainties in the isoprene oxidation mechanism impacts much of the work currently being pursued in the atmospheric community. Discrepancies in the modelled-to-measured OH concentration in isoprene rich environments can lead to overestimations of the methane lifetime and reduction in the rate of VOC degradation predicted by global models. Global or regional models currently able to reproduce isoprene observations likely underestimate the flux of BVOCs into the atmosphere; this underestimation will impact processes associated with their oxidation, for example, the formation of OVOCs, which can impact OH reactivity predictions and also SOA production, both of which are currently consistently underpredicted by atmospheric models in isoprene-rich environments. As carbonaceous aerosol strongly influences air quality and climate change, the accurate mechanism by which isoprene is oxidised to secondary gas-phase species and ultimately to SOA becomes increasingly sought.

Although earlier modelling studies often reduced isoprene emissions to reconcile the modelled isoprene mixing ratio with those observed, a number of observations of canopy scale fluxes have been reported which support the magnitude of isoprene emissions estimated by MEGAN. Perhaps as a consequence of this, the focus in more recent years has turned to the uncertainties associated with the isoprene oxidation mechanism itself rather than the estimated emissions. A number of alternative oxidation schemes have been proposed, some of which are able to reconcile the modelled OH radical concentration with observations (at times), for example the Leuven mechanism. It has been highlighted by recent laboratory studies, however, that the actual amount of OH recycled during isoprene oxidation may be lower than the Leuven mechanism predicts, and currently there does not seem to be one mechanism that can fully satisfy all field and laboratory based observations to date.

Uncertainty in the rate of deposition of isoprene oxidation products has also been suggested as a potential source of error in models. Increasing the rate of deposition of these species which act as important OH sinks could certainly extend the lifetime of OH and increase radical concentrations. There is no consensus in the current literature on how fast this deposition should be. Furthermore, increasing the deposition would only increase the discrepancy between OH reactivity observations and predictions. Although a bias in the measurement technique for OH could explain the large discrepancy between the direct OH observations and model predictions, this would not help to resolve the inconsistencies between observations and model predictions of the ratio of isoprene to its oxidation products, and also the disagreement between isoprene emission estimates based on satellite retrievals of HCHO columns and those predicted by the most recent emissions inventories. These discrepancies could certainly be improved, if not resolved, if mechanisms which generated more OH were implemented in atmospheric chemistry models [80, 81, 87] supporting the direct observations of OH.

References

1. Atkinson R, Baulch DL, Cox RA, Crowley JN, Hampson RF, Hynes RG, Jenkin ME, Rossi MJ, Troe J (2004) Evaluated kinetic and photochemical data for atmospheric chemistry: volume I – gas phase reactions of O_x, HO_x, NO_x and SO_x species. Atmos Chem Phys 4:1461–1738
2. Sander, S. P., J. Abbatt, J. R. Barker, J. B. Burkholder, R. R. Friedl, D. M. Golden, R. E. Huie, C. E. Kolb, M. J. Kurylo, G.K. Moortgat, V. L. Orkin and P. H. Wine "Chemical Kinetics and Photochemical Data for Use in Atmospheric Studies, Evaluation No. 17," JPL Publication 10-6, Jet Propulsion Laboratory, Pasadena, 2011 http://jpldataeval.jpl.nasa.gov.
3. Paulot F, Crounse JD, Kjaerdaard HG, Kroll JH, Seinfeld JH, Wennberg PO (2009) Isoprene photooxidation: new insights into the production of acids and organic nitrates. Atmos Chem Phys 9:1479–1501
4. Butler TM, Taraborrelli D, Brühl C, Fischer H, Harder H, Martinez M, Williams J, Lawrence MG, Lelieveld J (2008) Improved simulation of isoprene oxidation chemistry with the ECHAM5/MESSy chemistry-climate model: lessons from the GABRIEL airborne field campaign. Atmos Chem Phys 8:4529–4546
5. Carslaw N, Creasey DJ, Harrison D, Heard DE, Hunter MC, Jacobs PJ, Jenkin ME, Lee JD, Lewis AC, Pilling MJ, Saunders SM, Seakins PW (2001) OH and HO_2 radical chemistry in a forested region of north-western Greece. Atmos Environ 35:4725–4737
6. Hofzumahaus A, Rohrer F, Lu K, Bohn B, Brauers T, Chang CC, Fuchs H, Holland F, Kita K, Kondo Y, Li X, Lou S, Shao M, Zeng L, Wahner A, Zhang Y (2009) Amplified trace gas removal in the troposphere. Science 324:1702–1704
7. Kubistin D, Harder H, Martinez M, Rudolf M, Sander R, Bozem H, Eerdekens G, Fischer H, Gurk C, Klupfel T, Konigstedt R, Parchatka U, Schiller CL, Stickler A, Taraborrelli D, Williams J, Lelieveld J (2010) Hydroxyl radicals in the tropical troposphere over the Suriname rainforest: comparison of measurements with the box model MECCA. Atmos Chem Phys 10:9705–9728. doi:10.5194/acp-10-9705-2010
8. Lelieveld J, Butler TM, Crowley JN, Dillon TJ, Fischer H, Ganzeveld L, Harder H, Lawrence MG, Martinez M, Taraborrelli D, Williams J (2008) Atmospheric oxidation capacity sustained by a tropical forest. Nature 452:737–740

9. Martinez M, Harder H, Kubistin D, Rudolf M, Bozem H, Eerdekens G, Fischer H, Klupfel T, Gurk C, Konigstedt R, Parchatka U, Schiller CL, Stickler A, Williams J, Lelieveld J (2010) Hydroxyl radicals in the tropical troposphere over the Suriname rainforest: airborne measurements. Atmos Chem Phys 10:3759–3773. doi:10.5194/acp-10-3759
10. Ren X, Olson JR, Crawford J, Brune WH, Mao J, Long RB, Chen Z, Chen G, Avery MA, Sachse GW, Barrick JD, Diskin GS, Huey G, Fried A, Cohen RC, Heikes B, Wennberg PO, Singh HB, Blake D, Shetter R (2008) HO_x chemistry during INTEX-A 2004: observations, model calculation and comparison with previous studies. J Geophys Res Atmos 113:D05310
11. Stone D, Evans MJ, Edwards PM, Commane R, Ingham T, Rickard AR, Brookes DM, Hopkins J, Leigh RJ, Lewis AC, Monks PS, Oram D, Reeves CE, Stewart D, Heard DE (2011) Isoprene oxidation mechanisms: measurements and modelling of OH and HO(2) over a South-East Asian tropical rainforest during the OP3 field campaign. Atmos Chem Phys 11:6749–6771
12. Tan D, Faloona I, Simpas JB, Brune W, Shepson PB, Couch TL, Sumner AL, Carroll MA, Thornberry T, Apel E, Riemer D, Stockwell W (2001) HOx budgets in a deciduous forest: results from the PROPHET summer 1998 campaign. J Geophys Res Atmos 106: 24407–24427
13. Thornton JA, Wooldridge PJ, Cohen RC, Martinez M, Harder H, Brune WH, Williams EJ, Roberts JM, Fehsenfeld FC, Hall SR, Shetter RE, Wert BP, Fried A (2002) Ozone production rates as a function of NOx abundances and HOx production rates in the Nashville urban plume. J Geophys Res Atmos 107:4146
14. Whalley LK, Edwards PM, Furneaux KL, Goddard A, Ingham T, Evans MJ, Stone D, Hopkins JR, Jones CE, Karunaharan A, Lee JD, Lewis AC, Monks PS, Moller S, Heard DE (2011) Quantifying the magnitude of a missing hydroxyl radical source in a tropical rainforest. Atmos Chem Phys 11:7223–7233
15. Heard DE, Pilling MJ (2003) Measurement of OH and HO_2 in the troposphere. Chem Rev 103:5163–5198
16. Fuchs H, Bohn B, Hofzumahaus A, Holland F, Lu KD, Nehr S, Rohrer F, Wahner A (2010) Detection of HO_2 by laser-induced fluorescence: calibration and interferences from RO_2 radicals. Atmos Meas Tech 4:1209–1225
17. Mao J, Ren X, Brune W, Van Duin DM, Cohen RC, Park JH, Goldstein A, Paulot F, Beaver MR, Crounse JD, Wennberg PO, DiGangi JP, Henry SB, Keutsch FN, Park C, Schade GW, Wolfe GM, Thornton JA (2012) Insights into hydroxyl measurements and atmospheric oxidation in a California forest. Atmos Chem Phys Discuss 12:6715–6744
18. Creasey DJ, Heard DE, Lee JD (2001) OH and HO_2 measurements in a forested region of north-western Greece. Atmos Environ 35:4713–4724
19. Lelieveld J, Peters W, Dentener F, Krol MC (2002) Stability of tropospheric hydroxyl chemistry. J Geophys Res Atmos 107:4715
20. Lelieveld J, Dentener F, Peters W, Krol MC (2004) On the role of hydroxyl radicals in the self cleansing capacity of the troposphere. Atmos Chem Phys 4:2337–2344
21. Wang YH, Jacob DJ, Logan JA (1998) Global simulation of tropospheric O-3-NOx-hydrocarbon chemistry. 3. Origin of tropospheric ozone and effects of nonmethane hydrocarbons. J Geophys Res Atmos 103:10757–10767
22. Karl T, Guenther A, Turnipseed A, Tyndall G, Artaxo P, Martin S (2009) Rapid formation of isoprene photo-oxidation products observed in Amazonia. Atmos Chem Phys 9:7753–7767
23. Dillon TJ, Crowley JN (2008) Direct detection of OH formation in the reactions of HO_2 with $CH_3C(O)O_2$ and other substituted peroxy radicals. Atmos Chem Phys 8:4877–4889
24. Hasson AS, Tyndall GS, Orlando JJ (2004) A product yield study of the reaction of HO_2 radicals with ethyl peroxy ($C_2H_5O_2$), acetyl peroxy ($CH_3C(O)O_2$), and acetonyl peroxy ($CH_3C(O)CH_2O_2$) radicals. J Phys Chem A 108:5979–5989
25. Jenkin ME, Hurley MD, Wallington TJ (2007) Investigation of the radical product channel of the $CH_3C(O)O_2 + HO_2$ reaction in the gas phase. Phys Chem Chem Phys 9:3149–3162

26. Jenkin ME, Hurley MD, Wallington TJ (2008) Investigation of the radical product channel of the $CH_3C(O)$ CH_2O_2 + HO_2 reaction in the gas phase. Phys Chem Chem Phys 10:4274–4280
27. Jenkin ME, Hurley MA, Wallington TJ (2010) Investigation of the radical product channel of the $CH_3OCH_2O_2$ + HO_2 reaction in the gas phase. J Phys Chem A 114:408–416
28. Le Crane JP, Rayez MT, Rayez JC, Villenave E (2006) A reinvestigation of the kinetics and the mechanism of the CH3C(O)O-2 + HO_2 reaction using both experimental and theoretical approaches. Phys Chem Chem Phys 8:2163–2171
29. Pugh T, MacKenzie AR, Hewitt CN, Langford B, Edwards PM, Furneaux KL, Heard DE, Hopkins J, Jones CE, Karunaharan A, Lee JD, Mills G, Misztal P, Moller S, Monks PS, Whalley LK (2010) Simulating atmospheric composition over a South-East Asian tropical rainforest: performance of a chemistry box model. Atmos Chem Phys 10:279–298
30. Pugh TAM, MacKenzie AR, Langford B, Nemitz E, Misztal PK, Hewitt CN (2011) The influence of small-scale variations in isoprene concentrations on atmospheric chemistry over a tropical rainforest. Atmos Chem Phys 11:4121–4134
31. Hewitt CN, Lee JD, MacKenzie AR, Barkley MP, Carslaw N, Carver GD, Chappell NA, Coe H, Collier C, Commane R, Davies F, Davison B, Di Carlo P, Di Marco CF, Dorsey JR, Edwards PM, Evans MJ, Fowler D, Furneaux KL, Gallagher M, Guenther A, Heard DE, Helfter C, Hopkins J, Ingham T, Irwin M, Jones C, Karunaharan A, Langford B, Lewis AC, Lim SF, MacDonald SM, Mahajan AS, Malpass S, McFiggans G, Mills G, Misztal P, Moller S, Monks PS, Nemitz E, Nicolas-Perea V, Oetjen H, Oram DE, Palmer PI, Phillips GJ, Pike R, Plane JMC, Pugh T, Pyle JA, Reeves CE, Robinson NH, Stewart D, Stone D, Whalley LK, Yin X (2010) Overview: oxidant and particle photochemical processes above a south-east Asian tropical rainforest (the OP3 project): introduction, rationale, location characteristics and tools. Atmos Chem Phys 10:169–199
32. de Arellano JV-G, Patton EG, Karl T, van den Dries K, Barth MC, Orlando JJ (2011) The role of boundary layer dynamics on the diurnal evolution of isoprene and the hydroxyl radical over tropical forests. J Geophys Res Atmos 116:D07304
33. Dlugi R, Berger M, Zelger M, Hofzumahaus A, Siese M, Holland F, Wisthaler A, Grabmer W, Hansel A, Koppmann R, Kramm G, Mollmann-Coers M, Knaps A (2010) Turbulent exchange and segregation of HO_x radicals and volatile organic compounds above a deciduous forest. Atmos Chem Phys 10:6215–6235
34. Ouwersloot HG, de Arellano JV-G, van Heerwaarden CC, Ganzeveld LN, Krol MC, Lelieveld J (2011) On the segregation of chemical species in a clear boundary layer over heterogeneous land surfaces. Atmos Chem Phys 11:10681–10704
35. Paulot F, Crounse JD, Kjaergaard HG, Kurten A, St Clair JM, Seinfeld JH, Wennberg PO (2009) Unexpected epoxide formation in the gas-phase photooxidation of isoprene. Science 325:730–733
36. Carter WPL (1996) Condensed atmospheric photooxidation mechanisms for isoprene. Atmos Environ 30:4275–4290
37. Karl M, Dorn H-P, Holland F, Koppmann R, Poppe D, Rupp L, Schaub A, Wahner A (2006) Product study of the reaction of OH radicals with isoprene in the atmosphere simulation chamber SAPHIR. J Atmos Chem 55:167–187
38. Navarro MA, Dusanter S, Hites RA, Stevens PS (2011) Radical dependence of the yields of methacrolein and methyl vinyl ketone from the OH-initiated oxidation of Isoprene under NOx-free conditions. Environ Sci Technol 45:923–929
39. Saunders S, Jenkin M, Derwent R, Pilling M (2003) Protocol for the development of the Master Chemical Mechanism, MCM v3 (part A): tropospheric degradation of non-aromatic volatile organic compounds. Atmos Chem Phys 3:161–180
40. Da Silva G, Graham C, Wang Z-F (2010) Unimolecular beta-hydroxyperoxy radical decomposition with OH recycling in the photochemical oxidation of isoprene. Environ Sci Technol 44:250–256
41. Nguyen TL, Vereecken L, Peeters J (2010) HO(x) regeneration in the oxidation of isoprene III: theoretical study of the key isomerisation of the Z-delta-hydroxy-peroxy isoprene radicals. Chemphyschem 11:3996–4001

42. Peeters J, Nguyen TL, Vereecken L (2009) HO_x radical regeneration in the oxidation of isoprene. Phys Chem Chem Phys 11:5935–5939
43. Peeters J, Müller J-F (2010) HO(x) radical regeneration in isoprene oxidation via peroxy radical isomerisations. II. Experimental evidence and global impact. Phys Chem Chem Phys 12:14227–14235
44. Crounse JD, Knap HC, Ørnsø KB, Jørgensen S, Paulot F, Kjaerdaard HG, Wennberg PO (2012) Atmospheric fate of methacrolein 1 peroxy radical isomerization following addition of OH and O_2. J Phys Chem A 116(24):5756–5762
45. Taraborrelli D, Lawrence MG, Crowley JN, Dillon TJ, Gromov S, Groß CBM, Vereecken L, Lelieveld J (2012) Hydroxyl radical buffered by isoprene oxidation over tropical forests. Nat Geosci 5:190–193
46. Crounse JD, Paulot F, Kjaergaard HG, Wennberg PO (2011) Peroxy radical isomerization in the oxidation of isoprene. Phys Chem Chem Phys 13:13607–13613
47. Wolfe GM, Thornton JA, Bouvier-Brown NC, Goldstein AH, Park JH, McKay M, Matross DM, Mao J, Brune WH, LaFranchi BW, Browne EC, Min KE, Wooldridge PJ, Cohen RC, Crounse JD, Faloona IC, Gilman JB, Kuster WC, de Gouw JA, Huisman A, Keutsch FN (2011) The Chemistry of Atmosphere-Forest Exchange (CAFE) model – part 2: application to BEARPEX-2007 observations. Atmos Chem Phys 11:1269–1294
48. Archibald AT, Cooke MC, Utembe SR, Shallcross DE, Derwent RG, Jenkin ME (2010) Impacts of mechanistic changes on HO_x formation and recycling in the oxidation of isoprene. Atmos Chem Phys 10:8097–8118
49. Stavrakou T, Peeters J, Müller JF (2010) Improved global modelling of HO(x) recycling in isoprene oxidation: evaluation against the GABRIEL and INTEX-A aircraft campaign measurements. Atmos Chem Phys 10:9863–9878
50. Taraborrelli D, Lawrence MG, Butler TM, Sander R, Lelieveld J (2009) Mainz Isoprene Mechanism 2 (MIM2): an isoprene oxidation mechanism for regional and global atmospheric modelling. Atmos Chem Phys 9:2751–2777
51. Watson LA, Shallcross DE, Utembe SR, Jenkin ME (2008) A Common Representative Intermediates (CRI) mechanism for VOC degradation. Part 2: gas phase mechanism reduction. Atmos Environ 42:7196–7204
52. Edwards PM, Evans MJ, Stone D, Whalley LK, Furneaux KL, Hopkins J, Jones CE, Lewis AC, Heard DE (2011) Understanding missing OH sinks in a South East Asian tropical rainforest, Eos Transactions AGU, Fall Meeting Supplement 2011, Abstract B53A-06.
53. Emmerson KM, Evans MJ (2009) Comparison of tropospheric gas-phase chemistry schemes for use within global models. Atmos Chem Phys 9:1831–1845
54. Ingham T, Goddard A, Whalley LK, Furneaux KL, Edwards PM, Seal CP, Self DE, Johnson GP, Read KA, Lee JD, Heard DE (2009) A flow-tube based laser-induced fluorescence instrument to measure OH reactivity in the troposphere. Atmos Meas Tech 2:465–477
55. Elshorbany YF, Kleffmann J, Hofzumahaus A, Kurtenbach R, Wiesen P, Brauers T, Bohn B, Dorn HP, Fuchs H, Holland F, Rohrer F, Tillmann R, Wegener R, Wahner A, Kanaya Y, Yoshino A, Nishida S, Kajii Y, Martinez M, Kubistin D, Harder H, Lelieveld J, Elste T, Plass-Duelmer C, Stange G, Berresheim H, Schurath U (2012) HOx budgets during HOxComp: a case study of HO_x chemistry under NO_x-limited conditions. J Geophys Res Atmos 117: D03307
56. Kanaya Y, Hofzumahaus A, Dorn HP, Brauers T, Fuchs H, Holland F, Rohrer F, Bohn B, Tillmann R, Wegener R, Wahner A, Kajii Y, Miyamoto K, Nishida S, Watanabe K, Yoshino A, Kubistin D, Martinez M, Rudolf M, Harder H, Berresheim H, Elste T, Plass-Duelmer C, Stange G, Kleffmann J, Elshorbany Y, Schurath U (2012) Comparisons of observed and modeled OH and HO_2 concentrations during the ambient measurement period of the HO(x) Comp field campaign. Atmos Chem Phys 12:2567–2585
57. Lu K, Rohrer F, Holland F, Fuchs H, Bohn B, Brauers T, Chang CC, Haeseler R, Hu M, Kita K, Kondo Y, Li X, Lou S, Nehr S, Shao M, Zeng L, Wahner A, Zhang Y, Hofzumahaus A

(2012) Observations and modelling of OH and HO_2 concentrations in the Pearl River Delta 2006: a missing OH source in a VOC rich atmosphere. Atmos Chem Phys 12:1541–1569
58. Lu K, Hofzumahaus A, Holland F, Bohn B, Brauers T, Fuchs H, Hu M, Häseler R, Kita K, Kondo Y, Li X, Lou S, Oebel A, Shao M, Zeng L, Wahner A, Zhu T, Zhang Y, Rohrer F (2012) Missing OH source in a suburban environment near Beijing: observed and modelled OH and HO_2 concentrations in summer 2006. Atmos Chem Phys Discuss 12:10879–10936
59. Archibald AT, Levine JG, Abraham NL, Cooke MC, Edwards PM, Heard DE, Jenkin ME, Karunaharan A, Pike RC, Monks PS, Shallcross DE, Telford PJ, Whalley LK, Pyle JA (2011) Impacts of HO_x regeneration and recycling in the oxidation of isoprene: consequences for the composition of past, present and future atmospheres. Geophys Res Lett 38:L05804
60. Lamb B, Guenther A, Gay D, Westberg H (1987) A national inventory of biogenic hydrocarbon emissions. Atmos Environ 21:1695–1705
61. Müller JF (1992) Geographical-distribution and seasonal-variation of surface emissions and deposition velocities of atmospheric trace gases. J Geophys Res Atmos 97:3787–3804
62. Zimmerman P (1979) Testing of hydrocarbon emissions from vegetation, leaf litter and aquatic surfaces and development of a method for compiling biogenic emissions inventories. Environmental Protection Agency, EPA-450-4-70-004
63. Guenther A et al (1995) A global model of natural volatile organic compound emissions. J Geophys Res 100:8873–8892
64. Pierce TE, Waldruff PS (1991) Pc-Beis – a personal-computer version of the biogenic emissions inventory system. J Air Waste Manage Assoc 41:937–941
65. Pierce T, Geron C, Bender L, Dennis R, Tonnesen G, Guenther A (1998) Influence of increased isoprene emissions on regional ozone modeling. J Geophys Res Atmos 103:25611–25629
66. Guenther A, Karl T, Harley P, Wiedinmyer C, Palmer PI, Geron C (2006) Estimates of global terrestrial isoprene emissions using MEGAN (Model of Emissions of Gases and Aerosols from Nature). Atmos Chem Phys 6:3181–3210
67. Guenther A, Baugh B, Brasseur G, Greenberg J, Harley P, Klinger L, Serca D, Vierling L (1999) Isoprene emission estimates and uncertainties for the Central African EXPRESSO study domain. J Geophys Res Atmos 104:30625–30639
68. Harley P, Vasconcellos P, Vierling L, Pinheiro CCD, Greenberg J, Guenther A, Klinger L, De Almeida SS, Neill D, Baker T, Phillips O, Malhi Y (2004) Variation in potential for isoprene emissions among neotropical forest sites. Glob Change Biol 10:630–650
69. Keller M, Lerdau M (1999) Isoprene emission from tropical forest canopy leaves. Global Biogeochem Cycles 13:19–29
70. Kesselmeier J, Kuhn U, Wolf A, Andreae MO, Ciccioli P, Brancaleoni E, Frattoni M, Guenther A, Greenberg J, De Castro Vasconcellos P, de Telles Oliva T, Tavares T, Artaxo P (2000) Atmospheric volatile organic compounds (VOC) at a remote tropical forest site in central Amazonia. Atmos Environ 34:4063–4072
71. Klinger LF, Li QJ, Guenther AB, Greenberg JP, Baker B, Bai JH (2002) Assessment of volatile organic compound emissions from ecosystems of China. J Geophys Res Atmos 107:4603
72. Kuhn U, Rottenberger S, Biesenthal T, Ammann C, Wolf A, Schebeske G, Oliva ST, Tavares TM, Kesselmeier J (2002) Exchange of short-chain monocarboxylic acids by vegetation at a remote tropical forest site in Amazonia. J Geophys Res 107:8069. doi:10.1029/2000jd000303
73. Karl T, Guenther A, Spirig C, Hansel A, Fall R (2004) Seasonal variation of biogenic VOC emissions above a mixed hardwood forest in northern Michigan. Geophys Res Lett 30:2186
74. Karl T, Potosnak M, Guenther A, Clark D, Walker J, Herrick JD, Geron C (2004) Exchange processes of volatile organic compounds above a tropical rain forest: implications for modeling tropospheric chemistry above dense vegetation. J Geophys Res Atmos 109:D18306
75. Houweling S, Dentener F, Lelieveld J (1998) The impact of nonmethane hydrocarbon compounds on tropospheric photochemistry. J Geophys Res Atmos 103:10673–10696

76. Poisson N, Kanakidou M, Crutzen PJ (2000) Impact of non-methane hydrocarbons on tropospheric chemistry and the oxidizing power of the global troposphere: 3-dimensional modelling results. J Atmos Chem 36:157–230
77. Bey I, Aumont B, Toupance G (2001) A modeling study of the nighttime radical chemistry in the lower continental troposphere 2. Origin and evolution of HO_x. J Geophys Res 106:9991–10001
78. Ehhalt D, Prather M (2001) Atmospheric chemistry and greenhouse gases. In: Houghton J, Ding Y, Griggs D, Noguer M, van der Linden P, Xiaosu D (eds) Climate change 2001. Cambridge University Press, Cambridge
79. Spirig C, Neftel A, Ammann C, Dommen J, Grabmer W, Thielmann A, Schaub A, Beauchamp J, Wisthaler A, Hansel A (2005) Eddy covariance flux measurements of biogenic VOCs during ECHO 2003 using proton transfer reaction mass spectrometry. Atmos Chem Phys 5:465–481
80. Kuhn U, Andreae MO, Ammann C, Araujo AC, Brancaleoni E, Ciccioli P, Dindorf T, Frattoni M, Gatti LV, Ganzeveld L, Kruijt B, Lelieveld J, Lloyd J, Meixner FX, Nobre AD, Poschl U, Spirig C, Stefani P, Thielmann A, Valentini R, Kesselmeier J (2007) Isoprene and monoterpene fluxes from Central Amazonian rainforest inferred from tower-based and airborne measurements, and implications on the atmospheric chemistry and the local carbon budget. Atmos Chem Phys 7:2855–2879
81. Karl T, Guenther A, Yokelson RJ, Greenberg J, Potosnak M, Blake DR, Artaxo P (2007) The tropical forest and fire emissions experiment: emission, chemistry, and transport of biogenic volatile organic compounds in the lower atmosphere over Amazonia. J Geophys Res Atmos 112:D18302
82. Langford B, Misztal PK, Nemitz E, Davison B, Helfter C, Pugh TAM, MacKenzie AR, Lim SF, Hewitt CN (2010) Fluxes and concentrations of volatile organic compounds from a South-East Asian tropical rainforest. Atmos Chem Phys 10:8391–8412
83. Hewitt CN, Ashworth K, Boynard A, Guenther A, Langford B, MacKenzie AR, Misztal P, Nemitz E, Owen SM, Possell M, Pugh TAM, Ryan AC, Wild O (2011) Ground-level ozone influenced by circadian control of isoprene emissions. Nature Geoscience, ngeo 4:671–674
84. Fu TM, Jacob DJ, Palmer PI, Chance K, Wang YXX, Barletta B, Blake DR, Stanton JC, Pilling MJ (2007) Space-based formaldehyde measurements as constraints on volatile organic compound emissions in east and south Asia and implications for ozone. J Geophys Res Atmos 112:D06312
85. Millet DB, Jacob DJ, Boersma KF, Fu TM, Kurosu TP, Chance K, Heald CL, Guenther A (2008) Spatial distribution of isoprene emissions from North America derived from formaldehyde column measurements by the OMI satellite sensor. J Geophys Res Atmos 113:D02307
86. Shim C, Wang YH, Choi Y, Palmer PI, Abbot DS, Chance K (2005) Constraining global isoprene emissions with Global Ozone Monitoring Experiment (GOME) formaldehyde column measurements. J Geophys Res Atmos 110:D24301
87. Barkley MP, Palmer PI, Kuhn U, Kesselmeier J, Chance K, Kurosu TP, Martin RV, Helmig D, Guenther A (2008) Net ecosystem fluxes of isoprene over tropical South America inferred from Global Ozone Monitoring Experiment (GOME) observations of HCHO columns. J Geophys Res Atmos 113:D20304
88. Dibble TS (2004) Prompt chemistry of alkenoxy radical products of the double H-atom transfer of alkoxy radicals from isoprene. J Phys Chem A 108:2208–2215
89. Solomon SD, Qin D, Manning M, Alley RB, Berntsen T, Bindoff NL, Chen Z, Chidthaisong A, Gregory JM, Hegerl GC, Heimann M, Hewitson B, Hoskins BJ, Joos F, Jouzel J, Kattsov V, Lohmann U, Matsuno T, Molina M, Nicholls N, Overpeck J, Raga G, Ramaswamy V, Ren J, Rusticucci M, Somerville R, Stocker TF, Whetton P, Wood RA, Wratt D (2007) Climate change 2007: the physical science basis. Contribution of working group I to the fourth

assessment report of the Intergovernmental Panel on Climate Change IPCC. Cambridge University Press, Cambridge
90. Di Carlo P, Brune WH, Martinez M, Harder H, Lesher R, Ren X, Thornberry T, Carroll M, Young V, Shepson P, Riemer D, Apel E, Campbell C (2004) Missing OH reactivity in a forest: evidence for unknown reactive biogenic VOCs. Sci Mag 304:722–725
91. Kovacs TA, Brune WH, Harder H, Martinez M, Simpas JB, Frost GJ, Williams E, Jobson T, Stroud C, Young V, Fried A, Wert B (2003) Direct measurements of urban OH reactivity during Nashville SOS in summer 1999. J Environ Monit 5:68–74
92. Lee JD, McFiggans G, Allan JD, Baker AR, Ball SM, Benton AK, Carpenter LJ, Commane R, Finley BD, Evans MJ, Feuntes E, Furneaux KL, Goddard A, Good N, Hamilton JF, Heard DE, Herrmann H, Hollingsworth A, Hopkins JR, Ingham T, Irwin M, Jones CE, Jones RL, Keene WC, Lawler MJ, Lehmann S, Lewis AC, Long MS, Mahajan AS, Methven J, Moller SJ, Müller K, Müller T, Niedermeier N, O'Doherty S, Oetjen H, Plane JMC, Pszenny A, Read KA, Saiz-Lopez A, Saltzmann ES, Sander R, von Glasow R, Whalley LK, Wiedensohler A, Young D (2009) Reactive Halogens in the Marine Boundary Layer (RHaMBLe): the tropical North Atlantic experiments. Atmos Chem Phys Discuss 9:21717–21783
93. Lou S, Holland F, Rohrer F, Lu K, Bohn B, Brauers T, Chang CC, Fuchs H, Haeseler R, Kita K, Kondo Y, Li X, Shao M, Zeng L, Wahner A, Zhang Y, Wang W, Hofzumahaus A (2010) Atmospheric OH reactivities in the Pearl River Delta – China in summer 2006: measurement and model results. Atmos Chem Phys 10:11243–11260
94. Mao J, Ren X, Brune WH, Olson JR, Crawford JH, Fried A, Huey LG, Cohen RC, Heikes B, Singh HB, Blake DR, Sachse GW, Diskin GS, Hall SR, Shetter RE (2009) Airborne measurement of OH reactivity during INTEX-B. Atmos Chem Phys 9:163–173
95. Mogensen D, Smolander S, Sogachev A, Zhou L, Sinha V, Guenther A, Williams J, Nieminen T, Kajos MK, Rinne J, Kulmala M, Boy M (2011) Modelling atmospheric OH-reactivity in a boreal forest ecosystem. Atmos Chem Phys 11:9709–9719
96. Ren X, Harder H, Martinez M, Lesher R, Oliger A, Shirley T, Adams J, Simpas JB, Brune WH (2003) HO_x and OH reactivity observations in New York City during PMTACS-NY2001. Atmos Environ 37:3627–3637
97. Ren XR, Brune WH, Oliger A, Metcalf AR, Simpas JB, Shirley T, Schwab JJ, Bai CH, Roychowdhury U, Li YQ, Cai CX, Demerjian KL, He Y, Zhou XL, Gao HL, Hou J (2006) OH, HO_2, and OH reactivity during the PMTACS-NY Whiteface mountain 2002 campaign: observations and model comparison. J Geophys Res Atmos 111:D10S03
98. Sadanaga Y, Yoshino A, Kato S, Kajii Y (2005) Measurements of OH reactivity and photochemical ozone production in the urban atmosphere. Environ Sci Technol 39:8847–8852
99. Shirley TR, Brune WH, Ren X, Mao J, Lesher R, Cardenas B, Volkamer R, Molina LT, Molina MJ, Lamb B, Velasco E, Jobson T, Alexander M (2006) Atmospheric oxidation in the Mexico City Metropolitan Area (MCMA) during April 2003. Atmos Chem Phys 6:2753–2765
100. Sinha V, Williams J, Crowley JN, Lelieveld J (2008) The comparative reactivity method – a new tool to measure total OH reactivity in ambient air. Atmos Chem Phys 8:2213–2227
101. Sinha V, Williams J, Lelieveld J, Ruuskanen TM, Kajos MK, Patokoski J, Hellen H, Hakola H, Mogensen D, Boy M, Rinne J, Kulmala M (2010) OH reactivity measurements within a boreal forest: evidence for unknown reactive emissions. Environ Sci Technol 44:6614–6620
102. Lewis AC, Carslaw N, Marriott PJ, Kinghorn RM, Morrision P, Lee A, Bartle KD, Pilling MJ (2000) A larger pool of ozone-forming carbon compounds in urban atmospheres. Nature 405:778–781
103. Chung MY, Maris C, Krischke U, Meller R, Paulson SE (2003) An investigation of the relationship between total non-methane organic carbon and the sum of speciated hydrocarbons and carbonyls measured by standard GC/FID: measurements in the Los Angeles air basin. Atmos Environ 37:S159–S170

104. Warneke C, Gouw JAD (2001) Organic trace gas composition of the marine boundary layer over the northwest Indian Ocean in April 2000. Atmos Environ 35:5923–5933
105. Goldstein AH, Galbally IE (2007) Known and unexplored organic constituents in the Earth's atmosphere. Environ Sci Technol 41:1514–1521
106. Heald CL, Jacob DJ, Park RJ, Russell LM, Huebert BJ, Seinfeld JH, Liao H, Weber RJ (2005) A large organic aerosol source in the free troposphere missing from current models. Geophys Res Lett 32:L18809
107. Johnson D, Utembe SR, Jenkin ME, Derwent RG, Hayman GD, Alfarra MR, Coe H, McFiggans G (2006) Simulating regional scale secondary organic aerosol formation during the TORCH 2003 campaign in the southern UK. Atmos Chem Phys 6:403–418
108. Morris RE, McNally DE, Tesche TW, Tonnesen G, Boylan JW, Brewer P (2005) Preliminary evaluation of the community multiscale air, quality model for 2002 over the southeastern United States. J Air Waste Manage Assoc 55:1694–1708
109. Morris RE, Koo B, Guenther A, Yarwood G, McNally D, Tesche TW, Tonnesen G, Boylan J, Brewer P (2006) Model sensitivity evaluation for organic carbon using two multi-pollutant air quality models that simulate regional haze in the southeastern United States. Atmos Environ 40:4960–4972
110. Volkamer R, Jimenez JL, San Martini F, Dzepina K, Zhang Q, Salcedo D, Molina LT, Worsnop DR, Molina MJ (2006) Secondary organic aerosol formation from anthropogenic air pollution: rapid and higher than expected. Geophys Res Lett 33:L17811
111. Yu SC, Mathur R, Schere K, Kang DW, Pleim J, Young J, Tong D, Pouliot G, McKeen SA, Rao ST (2008) Evaluation of real-time PM(2.5) forecasts and process analysis for PM(2.5) formation over the eastern United States using the Eta-CMAQ forecast model during the 2004 ICARTT study. J Geophys Res Atmos 113:D06204
112. Pandis SN, Paulson SE, Seinfeld JH, Flagan RC (1991) Aerosol formation in the photooxidation of isoprene and beta-pinene. Atmos Environ A Gen Top 25:997–1008
113. Kamens RM, Gery MW, Jeffries HE, Jackson M, Cole EI (1982) Ozone-isoprene reactions – product formation and aerosol potential. Int J Chem Kinet 14:955–975
114. Miyoshi A, Hatakeyama S, Washida N (1994) Om radical-initiated photooxidation of isoprene – an estimate of global co production. J Geophys Res Atmos 99:18779–18787
115. Pankow JF (1994) An absorption-model of gas-particle partitioning of organic-compounds in the atmosphere. Atmos Environ 28:185–188
116. Kiendler-Scharr A, Wildt J, Dal Maso M, Hohaus T, Kleist E, Mentel TF, Tillmann R, Uerlings R, Schurr U, Wahner A (2009) New particle formation in forests inhibited by isoprene emissions. Nature 461:381–384
117. Chan M, Surratt JD, Claeys M, Edgerton ES, Tanner RL, Shaw SL, Zheng M, Knipping EM, Eddingsaas NC, Wennberg PO, Seinfeld JH (2010) Characterisation and quantification of isoprene-derived epoxydiolsin ambient aerosol in the southeastern United States. Environ Sci Technol 44:4590–4596
118. Claeys M, Graham B, Vas G, Wang W, Vermeylen R, Pashynska V, Cafmeyer J, Guyon P, Andreae MO, Artaxo P, Maenhaut W (2004) Formation of secondary organic aerosols through photooxidation of isoprene. Science 303:1173–1176
119. Claeys M, Wang W, Ion AC, Kourtchev I, Gelencser A, Maenhaut W (2004) Formation of secondary organic aerosols from isoprene and its gas-phase oxidation products through reaction with hydrogen peroxide. Atmos Environ 38:4093–4098
120. Ion AC, Vermeylen R, Kourtchev I, Cafmeyer J, Chi X, Gelencser A, Maenhaut W, Claeys M (2005) Polar organic compounds in rural PM2.5 aerosols from K-puszta, Hungary, during a 2003 summer field campaign: sources and diurnal variations. Atmos Chem Phys 5:1805–1814
121. Kourtchev I, Ruuskanen T, Maenhaut W, Kulmala M, Claeys M (2005) Observations of 2-methyltetrols and related photo-oxidation products of isoprene in boreal forest aerosols from Hyytiala, Finland. Atmos Chem Phys 5:2761–2770
122. Matsunaga S, Mochida M, Kawaamura K (2003) Growth of organic aerosol by biogenic semi-volatile carbonyls in the forestal atmosphere. Atmos Environ 37:2045–2050

123. Surratt JD, Gomez-Gonzalez Y, Chan AWH, Vermeylen R, Shahgholi M, Kleindienst TE, Edney EO, Offenberg JH, Lewandowski M, Jaoui M, Maenhaut W, Claeys M, Flagan RC, Seinfeld JH (2008) Organosulphate formation in biogenic secondary organic aerosol. J Phys Chem A 112:8345–8378
124. Odum JR, Hoffmann T, Bowman F, Collins D, Flagan RC, Seinfeld JH (1996) Gas/particle partitioning and secondary organic aerosol yields. Environ Sci Technol 30:2580–2585
125. Limbeck A, Kulmala M, Puxbaum H (2003) Secondary organic aerosol formation in the atmosphere via heterogeneous reaction of gaseous isoprene on acidic particles. Geophys Res Lett 30:1996
126. Dommen J, Metzger A, Duplissy J, Kalberer M, Alfarra MR, Gascho A, Weingartner E, Prevot ASH, Verheggen B, Baltensperger U (2006) Laboratory observation of oligomers in the aerosol from isoprene/NOx photooxidation. Geophys Res Lett 33:L13805
127. Kroll JH, Ng NL, Murphy SM, Flagan RC, Seinfeld JH (2005) Secondary organic aerosol formation from isoprene photooxidation under high-NOx conditions. Geophys Res Lett 32: L18808
128. Kroll JH, Ng NL, Murphy SM, Flagan RC, Seinfeld JH (2006) Secondary organic aerosol formation from isoprene photooxidation. Environ Sci Technol 40:1869–1877
129. Ng NL, Kroll JH, Keywood MD, Bahreini R, Varutbangkul V, Flagan RC, Seinfeld JH, Lee A, Goldstein AH (2006) Contribution of first- versus second-generation products to secondary organic aerosols formed in the oxidation of biogenic hydrocarbons. Environ Sci Technol 40:2283–2297
130. Kleindienst TE, Lewandowski M, Offenberg JH, Jaoui M, Edney EO (2009) The formation of secondary organic aerosol from isoprene + OH reaction in the absence of NO_x. Atmos Chem Phys 9:6541–6558
131. Surratt JD, Murphy SM, Kroll JH, Ng NL, Hildebrandt L, Sorooshian A, Szmigielski R, Vermeylen R, Maenhaut W, Claeys M, Flagan RC, Seinfeld JH (2006) Chemical composition of secondary organic aerosol formed from the photooxidation of isoprene. J Phys Chem A 110:9665–9690
132. Surratt JD, Chan AWH, Eddingsaas NC, Chan M, Loza CL, Kwan AJ, Hersey SP, Flagan RC, Wennberg PO, Seinfeld JH (2010) Atmospheric chemistry special feature: reactive intermediates revealed in secondary organic aerosol formation from isoprene. Proc Natl Acad Sci USA 107(15):6640–6645
133. Kiendler-Scharr A, Andres S, Bachner M, Behnke K, Broch S, Hofzumahaus A, Holland F, Kleist E, Mentel TF, Rubach F, Springer M, Steitz B, Tillmann R, Wahner A, Schnitzler JP, Wildt J (2012) Isoprene in poplar emissions: effects on new particle formation and OH concentrations. Atmos Chem Phys 12:1021–1030
134. Robinson NH, Hamilton JF, Allan JD, Langford B, Oram DE, Chen Q, Docherty K, Farmer DK, Jimenez JL, Ward MW, Hewitt CN, Barley MH, Jenkin ME, Rickard AR, Martin ST, McFiggans G, Coe H (2011) Evidence for a significant proportion of Secondary organic aerosol from isoprene above a maritime tropical forest. Atmos Chem Phys 11:1039–1050
135. Froyd KD, Murphy SM, Murphy DM, de Gouw JA, Eddingsaas NC, Wennberg PO (2010) Contribution of isoprene-derived organosulfates to free tropospheric aerosol mass. Proc Natl Acad Sci USA 107:21360–21365
136. Henze DK, Seinfeld JH (2006) Global secondary organic aerosol from isoprene oxidation. Geophys Res Lett 33:L09812
137. Carlton AG, Wiedinmyer C, Kroll JH (2009) A review of Secondary Organic Aerosol (SOA) formation from isoprene. Atmos Chem Phys 9:4987–5005
138. Olson JR, Crawford JH, Davis DD, Chen G, Avery MA, Barrick JDW, Sachse GW, Vay SA, Sandholm ST, Tan D, Brune WH, Faloona IC, Heikes BG, Shetter RE, Lefer BL, Singh HB, Talbot RW, Blake DR (2001) Seasonal differences in the photochemistry of the South Pacific: a comparison of observations and model results from PEM-Tropics A and B. J Geophys Res 106:32749–32766

http://www.springer.com/978-3-642-41214-1

Atmospheric and Aerosol Chemistry

McNeill, V.F.; Ariya, P.A. (Eds.)
2014, VII, 264 p. 63 illus., 26 illus. in color., Hardcover
ISBN: 978-3-642-41214-1